Mixed-State Long-Range Order and Criticality from Measurement and Feedback

Tsung-Cheng Lu,[1,*] Zhehao Zhang,[2,†] Sagar Vijay,[2,‡] and Timothy H. Hsieh[1,§]

[1] *Perimeter Institute for Theoretical Physics, Waterloo, Ontario N2L 2Y5, Canada*

[2] *Department of Physics, University of California, Santa Barbara, California 93106, USA*

(Received 1 May 2023; revised 13 July 2023; accepted 17 July 2023; published 7 August 2023)

We propose a general framework for using local measurements, local unitaries, and nonlocal classical communication to construct quantum channels, which can efficiently prepare mixed states with long-range quantum order or quantum criticality. As an illustration, symmetry-protected topological phases can be universally converted into mixed states with long-range entanglement, which can undergo phase transitions with quantum critical correlations of local operators and a logarithmic scaling of the entanglement negativity, despite coexisting with volume-law entropy. Within the same framework, we present two applications using fermion occupation-number measurement to convert (i) spinful free fermions in one dimension into a quantum critical mixed state with enhanced algebraic correlations between spins and (ii) Chern insulators into a mixed state with critical quantum correlations in the bulk. The latter is an example where mixed-state quantum criticality can emerge from a gapped state of matter in constant depth using local quantum operations and nonlocal classical communication.

DOI: 10.1103/PRXQuantum.4.030318

I. INTRODUCTION

Interacting quantum matter may exhibit long-range entanglement that is intimately connected to fascinating phenomena such as fractionalized quasiparticles and criticality. Typically the scope for exploring long-range entanglement has been limited to pure states, especially the ground states of many-body Hamiltonians. However, realistic physical systems require a mixed-state description due to constant exposure to an environment, thus motivating the consideration of long-range entanglement in many-body mixed states. In equilibrium, mixed states naturally arise as finite-temperature Gibbs states; however, long-range entanglement is typically fragile to thermal fluctuations [1–5]. In contrast, out-of-equilibrium mixed states offer richer possibilities for stabilizing long-range entanglement. For example, there has been substantial recent progress in characterizing universal properties of various nontrivial states of matter, e.g., symmetry-protected topological (SPT) phases, quantum critical states, and topological order, subject to noise channels [6–14]. Signatures of the non-trivial nature of these mixed-states generally require probing nonlinear observables in the mixed-state density matrix, e.g., measures of quantum entanglement.

In this work, we introduce a novel route for realizing long-range entangled mixed states. We provide a general framework for constructing quantum channels, which allow for the efficient realization of a large class of mixed-state long-range entanglement, including GHZ, topological order, and quantum criticality. Specifically, our protocols generate pure states with certain probabilities, hence defining a mixed-state ensemble. Importantly, the long-range order and criticality can be efficiently probed through observables that are linear in the mixed-state density matrix.

Our construction (Sec. II, see Fig. 1 for schematic) relies on three ingredients, namely, local projective measurement, local unitary operations, and nonlocal classical communication. Starting with an input state, which we extensively bipartition in two disjoint Hilbert spaces, A and B, we perform single-site measurements within A. Based on the measurement outcomes, recorded as classical data, we perform appropriate unitary feedback consisting of local unitary gates acting on B. We will allow the local unitary gates to depend on the *global* classical data, thus requiring nonlocal classical communication. Such a two-step protocol generically generates an ensemble of pure states associated with distinct measurement outcomes, hence defining a mixed state. The resulting mixed

*tlu@perimeterinstitute.ca
†zhehao@umail.ucsb.edu
‡sagar@physics.ucsb.edu
§thsieh@perimeterinstitute.ca

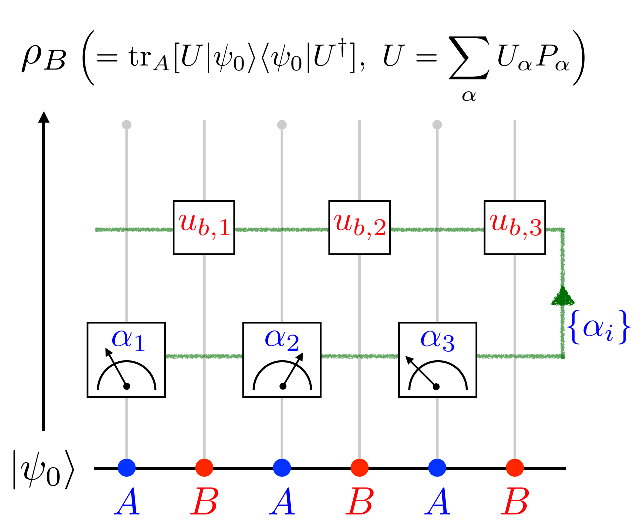

FIG. 1. We consider a system with A, B degrees of freedom, which may correspond to sublattices or charge and spin of fermions, for example. We devise a depth-2 quantum channel that can effectively implement a controlled unitary, giving rise to various long-range quantum orders and criticality on the B system. The first layer consists of single-site measurements on A, and the second layer consists of single-site unitaries on B conditioned on the outcomes $\{\alpha\}$ in the first layer. This protocol outputs a density matrix ρ_B on B such that $\rho_B(= \mathrm{tr}_A\,|\psi\rangle\,\langle\psi|)$ admits a purification $|\psi\rangle = U\,|\psi_0\rangle$ with U being a controlled unitary $U = \sum_\alpha U_\alpha P_\alpha$ on an AB composite system; P_α projects A to a specific product state on A, and U_α is a product of on-site unitaries acting on B.

state on B (ρ_B) may exhibit various long-range quantum orders and quantum criticality coexisting with extensive classical entropy. We show that ρ_B admits a purification that can be obtained by performing a controlled unitary on the composite AB system. As such, our protocol may be regarded as implementing a controlled unitary that generically cannot be realized using finite-depth unitary circuits. This unitary description also provides a powerful handle allowing us to characterize ρ_B by analyzing the parent Hamiltonian of its purification.

Our framework is inspired by adaptive circuits, where the choice of the applied local unitary gates depends on the global measurement outcomes in a way that postmeasurement pure-state trajectories associated with different measurement outcomes will be deterministically converted to the same target pure state. This architecture has provided a powerful framework that enables the efficient preparation of a large class of nontrivial pure states, including gapped topological orders and gapless conformal critical states in short times [15–25], which are impossible using any local unitary protocols. The operations required by adaptive circuits (midcircuit measurements and feedback) are available in several quantum hardwares, and indeed the adaptive, finite-depth preparation of certain topological orders has been realized experimentally in recent works [26,27]. While our construction of quantum channels utilizes the same ingredients (local quantum operations and nonlocal classical communication) as in adaptive circuits, various postmeasurement states generically do not converge in our protocol, thereby leading to a mixed-state ensemble that exhibits certain long-range quantum order and quantum criticality despite having extensive entropy.

For the applications discussed in this work, the unitary feedback after local measurements is a product of onsite unitary operations, and hence, the long-range order in the resulting ensemble may equivalently be decoded from postmeasurement pure-state trajectories via appropriate classical postprocessing without unitary feedback (see, e.g., Refs. [28,29]). However, our protocol can be generalized, e.g., by extending onsite-unitary feedback to a finite-depth local unitary circuit, or by considering multiple rounds of layers of measurement and unitary. In both cases, it is unclear if the properties of the resulting mixed state can be efficiently obtained by classical postprocessing based on local measurement data. Furthermore, not all classical postprocessing can be implemented efficiently as quantum channels.

In the rest of the Introduction, we provide an overview of two classes of applications. The first class of examples takes a SPT order as an input state (Sec. IV). These are short-range entangled phases that can be prepared from product states using local unitary in finite time only when breaking the protecting symmetry [30,31]. We will focus on SPT phases characterized by decorated domain-wall constructions [32]. One class of examples are SPT phases in d-spatial dimensions, which are protected by $\mathbb{Z}_2$ p-form $\times\mathbb{Z}_2$ q-form symmetry with $p+q=d-1$. This type of SPT can be diagnosed by the long-range order in certain nonlocal operators, e.g., string operators in one dimension (1D) or membrane operators in two dimensions (2D). Based on these nonlocal operators, we show how to employ measurement and feedback to prepare a mixed state with $\mathbb{Z}_2$ long-range order coexisting with volume-law entropy. For instance, $\mathbb{Z}_2$ cat-state order and $\mathbb{Z}_2$ topological order can be prepared in one and two space dimensions in a mixed state, both of which cannot occur in equilibrium thermal states.

Notably, the convertibility to a long-range order is a universal property of the SPT: any pure state in the same SPT phase always leads to a long-range-ordered (and generically mixed) state characterized by the same universal properties that are related to the SPT order. In addition, the output state is a reduced density matrix of a ground state of Hamiltonian H that is “dual” to the parent Hamiltonian H_0 of the input SPT. Most interestingly, when H_0 is tuned to criticality, H is critical as well, and the corresponding mixed state possesses a critical entanglement structure quantified by the entanglement negativity [33–37]. For example, our protocol in 1D gives rise to a mixed state with volume-law scaling of von Neumann entropy, but logarithmic scaling of the entanglement negativity with subsystem size. Such mixed-state quantum criticality presents several unconventional features as we will discuss in this work.

Our application of converting a $\mathbb{Z}_2 \times \mathbb{Z}_2$ SPT to long-range order is directly inspired by Refs. [15,16,20]. In particular, Ref. [20] argues that measuring these SPTs will generically lead to certain long-range order in postmeasurement pure-state trajectories. While this can be shown analytically for fixed-point SPTs [15,16], the fate of SPTs away from fixed points upon measurement was inconclusive [38]. In contrast, our channel-based approach allows us to show that the emergence of long-range orders *in a mixed state* is a universal property that persists throughout the entire SPT phase. Importantly, these orders can be efficiently probed through certain linear observables in the mixed-state ensemble that results from our quantum channel.

The second class of examples focuses on spinful fermionic systems (Sec. V). We consider extensive single-site fermion occupation-number measurement followed by unitary feedback according to the measurement outcomes. In contrast to the single-site projective Pauli measurement, which trivializes the measured qubit, the occupation number for spinful fermions allows for richer phenomenology due to the possibility of a residual spin-1/2 degree of freedom in the subspace of a singly occupied site. Indeed, it is known that starting with noninteracting spinful fermions, performing a Gutzwiller projection (projecting onto single-occupation subspace) effectively induces interactions that may lead to various exotic quantum spin liquids in two and higher spatial dimensions (see Refs. [39,40] for reviews). The Gutzwiller projection cannot be implemented as a fermion occupation-number measurement, without postselecting the measurement outcome. In contrast, our scheme does not rely on postselection; for each postmeasurement trajectory, we apply a depth-1 local unitary feedback, so that the mixed state, formed from the ensemble of these trajectories, exhibits certain nontrivial features. We also note that the fermion-occupation-number measurement is readily experimentally available via quantum gas microscopes (see Ref. [41] for a review), which allows for the implementation of our protocols. Below we briefly summarize two applications, in one and two space dimensions, respectively.

In 1D, we start from free spinful fermions (Sec. V A) with nearest-neighbor hopping. In this case, it is known that spin-spin correlations decay algebraically with the separation between two sites with an exponent 2. We devise a protocol that outputs a mixed state with an enhanced critical correlation characterized by a smaller exponent, namely, 1. The essential idea is to notice that there is a long-range string order in the 1D free fermions [42], and measurement and feedback can convert this hidden string order into a truly long-range critical order. The resulting mixed state that describes correlations in the spin sector can be regarded as a reduced density matrix by tracing out the charge sector in a ground state of a parent Hamiltonian that we derive. Notably, this Hamiltonian describes strongly interacting spinful fermions and therefore, our measurement-feedback channel may be viewed as a novel means to effectively engineer interactions. We note that our protocol of boosting critical correlations is also applicable to interacting fermionic systems characterized by Luttinger liquids by exploiting their hidden string order.

The 2D example (Sec. V B) takes Chern insulators (see, e.g., Ref. [43] for an Introduction) as an input. These are gapped invertible topological phases, which feature trivial bulks and nontrivial chiral edge modes on the boundary. Despite Chern insulators having exponentially decaying correlations in the bulk, applying a measurement-feedback channel leads to a mixed state with algebraic correlations. The essential property we use is a nonlocal membrane order parameter due to the topological response in Chern insulating states [44,45]. Such a nonlocal hidden order can be converted into algebraic decaying spin-spin correlations in the resulting mixed state using a nonlocal quantum channel. This, therefore, furnishes a remarkable example where quantum criticality emerges from a gapped state of matter via a quantum channel involving local quantum operations but nonlocal classical communication.

II. NONLOCAL CHANNEL FROM LOCAL QUANTUM OPERATIONS AND NONLOCAL CLASSICAL COMMUNICATION

Here we introduce the protocol for constructing quantum channels based on local quantum operations (measurement and unitary) and nonlocal classical communication (Fig. 1). Given a system with two types of degrees of freedom A and B initialized in the state $\rho_0 = |\psi_0\rangle\langle\psi_0|$, one performs simultaneous, extensive single-site measurement on every degree of freedom in A. This leads to a particular pure state $|\psi_\alpha\rangle = P_\alpha |\psi_0\rangle / \sqrt{\langle\psi_0| P_\alpha |\psi_0\rangle}$ with probability $\langle\psi_0| P_\alpha |\psi_0\rangle$, where α labels the measurement outcome on A, and P_α is the projector associated with the measurement. For each postmeasurement state, we apply a unitary U_α acting on B based on the outcome α. Note that this requires nonlocal classical communication since the choice of a local unitary relies on distant measurement outcomes recorded as classical data. The above measurement-feedback protocol leads to a mixed state

$$\rho = \sum_\alpha U_\alpha P_\alpha \rho_0 P_\alpha U_\alpha^\dagger. \tag{1}$$

With an appropriate choice of measurement and unitary feedback, the subsystem B described by a reduced density matrix ρ_B may exhibit various long-range quantum orders and criticality.

The aforementioned protocol may be viewed as a way to effectively implement a controlled unitary acting on the AB composite system followed by tracing out A. To see this, we notice that ρ_B admits a purification $|\psi\rangle$ via $\rho_B = \mathrm{tr}_A |\psi\rangle\langle\psi|$, where $|\psi\rangle$ is defined as

$$|\psi\rangle = \sum_\alpha U_\alpha P_\alpha |\psi_0\rangle . \quad (2)$$

$U = \sum_\alpha U_\alpha P_\alpha$ takes the form of a controlled unitary with A being the control and B being the target. U may not be realized as local unitary circuits, thereby enabling significant changes in the entanglement structure. In particular, U provides a nonlocal transformation on operators according to Heisenberg evolution. For instance, the expectation of an operator O_B supported on B in the resulting mixed state ρ_B amounts to the expectation of the operator $U^\dagger O_B U$ in the input pure state $|\psi_0\rangle$. As such, this nonlocal unitary transformation provides a powerful way to convert hidden orders in the input state into long-range order or criticality in the density matrix ρ_B, as we will illustrate using various examples. Moreover, this viewpoint of unitary transformation provides a useful way to describe the output ρ_B; since the initial state $|\psi_0\rangle$ and the purified state $|\psi\rangle$ are connected by a unitary U, the structure of ρ_B can be characterized based on the Hamiltonian H of $|\psi\rangle$ through $H = UH_0U^\dagger$, where H_0 is the Hamiltonian of the input state $|\psi_0\rangle$.

III. ENTANGLEMENT STRUCTURE OF OUTPUT MIXED STATES

We first discuss general constraints on the entanglement properties of the mixed states generated from such protocols.

Bound on entanglement: the protocols presented in this work belong to LOCC, namely, local operations (onsite measurement and unitaries) and classical communication, and therefore, mixed-state entanglement cannot increase under these quantum channels (see Appendix A for proof based on the entanglement of formation [46], a faithful entanglement measure for mixed states). This entanglement constraint provides a sharp distinction between the mixed-state orders that may and may not be realized within our protocols. For example, starting with an area-law entangled gapped state in 1D, our finite-depth channels cannot output a mixed state with $\log L$ scaling entanglement. Namely, to output a quantum critical mixed state in 1D with $\log L$ scaling entanglement, the initial state must be critical with entanglement $\gtrsim O(\log L)$ as well, and Sec. IV C presents one such example. On the other hand, if one starts with a gapped, area-law state in 2D, the entanglement constraint does not rule out the possibility of realizing quantum critical mixed states (recall gapless conformal critical states obey an area law as well), and indeed this is realized in Sec. V B.

Sufficient conditions for a nontrivial mixed state: despite the above constraint on the quantity of entanglement, our protocol can produce mixed states ρ that are long-range entangled in the precise sense that they cannot be a mixture of trivial pure states [2]. Namely, ρ is long-range entangled if $\rho \neq \sum_n p_n |\phi_n\rangle\langle\phi_n|$, where each $|\phi_n\rangle$ is a short-range entangled state that can be connected to a product state using a finite-time local unitary [47].

We prove that ρ cannot be a mixture of short-range entangled states given the following two conditions (which will apply to all examples considered in this work). (i) *Global symmetry:* there exists a unitary operator S with unit-norm expectation value, i.e., $\mathrm{tr}(\rho S) = e^{i\theta}$ with $\theta \in \mathbb{R}$. (ii) *Long-range correlations for charged operators:* there exist charged operators O_1, O_2 (with respect to the symmetry S) [48], whose correlation $\mathrm{tr}(\rho O_1 O_2)$ decay slower than $e^{-d/\xi}$, with $\xi > 0$, and d being the spatial separation between O_1 and O_2. For example, $\mathrm{tr}(\rho O_1 O_2)$ could be constant or follow a power-law decay with the separation d.

The claim above can be proved by contradiction. Assume $\rho = \sum_n p_n |\phi_n\rangle\langle\phi_n|$, i.e., a mixture of short-range entangled pure states $|\phi_n\rangle$. Since $\mathrm{tr}(\rho S) = e^{i\theta}$, it must be that $\langle\phi_n|S|\phi_n\rangle = e^{i\theta}$ for each $|\phi_n\rangle$ [49]. Further, $|\phi_n\rangle$ being short-range entangled means the connected correlation function decays exponentially: $\langle\phi_n|O_1O_2|\phi_n\rangle - \langle\phi_n|O_1|\phi_n\rangle\langle\phi_n|O_2|\phi_n\rangle \sim e^{-d/\xi_n}$ [50] with ξ_n upper bounded by a finite $\xi_{\max}$. $\langle\phi_n|S|\phi_n\rangle = e^{i\theta}$ and the assumption that each operator is charged with respect to S implies that $\langle\phi_n|O_1|\phi_n\rangle = \langle\phi_n|O_2|\phi_n\rangle = 0$, and thus $\langle\phi_n|O_1O_2|\phi_n\rangle \sim e^{-d/\xi_n}$. Since O_1O_2 decays exponentially in each $|\phi_n\rangle$, O_1O_2 must decay exponentially in the mixed-state ensemble ρ, which contradicts the result that the decay of $\mathrm{tr}(\rho O_1 O_2)$ is slower than exponential. As a result, the initial assumption must be false.

As a demonstration, when the expectation value of a global $\mathbb{Z}_2$ symmetry generator follows $\langle S\rangle = \left\langle\prod_i X_i\right\rangle = 1$ in the mixed state, Z_iZ_j having nonzero expectation value as the separation $d \to \infty$ implies a nontrivial mixed state with the GHZ-type order. Such an example will be presented in Sec. IV A. If Z_iZ_j instead decays algebraically, the corresponding nontrivial mixed state exhibits a quantum criticality with several unconventional properties, which will be discussed in Sec. IV C. One may also generalize S and charged operators O_j to stringlike operators, which can witness mixed-state topological order in two space dimensions (see Appendix C for details).

IV. MIXED-STATE LONG-RANGE ORDER BY MEASURING SPT PHASES

In this section, we apply the general framework discussed in Sec. II to convert SPT phases characterized by decorated domain-wall construction [32] to mixed-state long-range orders. We will illustrate the main idea using 1D $\mathbb{Z}_2 \times \mathbb{Z}_2$ SPT. More general types of SPTs with distinct symmetries or higher-space dimensions and the corresponding emergent long-range order will be briefly outlined in Sec. IV D (with more details in the Appendix).

We also note that Refs. [28,29] discussed a protocol that can convert certain SPTs to a mixed-state ensemble with hidden long-range orders that can be decoded via nonlinear observables or classical postprocessing. However, the specific protocol is different from ours, and thus the type of long-range order that can be stabilized also differs. For example, our setup can realize GHZ-type order in 1D and $\mathbb{Z}_2$ topological order in 2D, both of which are absent in those works. More technically, the protocol discussed in Refs. [28,29] amounts to introducing thermal fluctuations, which is a qualitatively different perturbation than the ones we consider.

A. Measuring 1D SPT

We consider a 1D lattice with periodic boundary conditions, and the lattice sites are labeled with the ordering $(a,1),(b,1),(a,2),(b,2),\ldots,(a,L),(b,L)$. The cluster state Hamiltonian is defined as $-\sum_{i=1}^{L}(Z_{a,i}X_{b,i}Z_{a,i+1} + Z_{b,i}X_{a,i+1}Z_{b,i+1})$. The ground state exhibits an SPT order protected by the global $\mathbb{Z}_2 \times \mathbb{Z}_2$ symmetry generated by $\prod_{i=1}^{L} X_{a,i}$ on A sublattice and $\prod_{i=1}^{L} X_{b,i}$ on B sublattice. Under symmetric local perturbations without gap closing, the SPT order is robust in the ground state $|\psi_0\rangle$, and can be diagnosed by the long-range string order (see, e.g., Ref. [51])

$$\langle\psi_0|\, Z_{b,i}\left(\prod_{k=i+1}^{j} X_{a,k}\right) Z_{b,j}\,|\psi_0\rangle = c \tag{3}$$

with $0 < c \le 1$ as $|i-j| \to \infty$ [52].

Now we show that based on the long-range string order, one can prepare a mixed state with GHZ-like $\mathbb{Z}_2$ symmetry-breaking order using measurement and unitary feedback in constant depth.

To start, we measure Pauli X for every site in A sublattice and denote the measurement outcome of $X_{a,i}$ by α_i. Defining $\alpha = \{\alpha_i\}$ as the collection of outcomes, one obtains a postmeasurement state $P_\alpha |\psi_0\rangle/\sqrt{\langle\psi_0| P_\alpha |\psi_0\rangle}$ with probability $p_\alpha = \langle\psi_0| P_\alpha |\psi_0\rangle$ and projector $P_\alpha \equiv \prod_i (1+\alpha_i X_{a,i})/2$. Without recording the outcome, the system is described by a mixed state, i.e., an ensemble of pure states corresponding to distinct measurement outcomes: $\sum_\alpha P_\alpha \rho_0 P_\alpha$ with $\rho_0 = |\psi_0\rangle\langle\psi_0|$. This measurement-induced ensemble lacks any long-range order. For instance, the two-point functions on B sublattice with respect to the mixed state is $\langle\psi_0| Z_{b,i} Z_{bj} |\psi_0\rangle$, which is nothing but the two-point functions with respect to the initial SPT, therefore decaying exponentially with the separation.

In contrast, applying unitary feedback based on the measurement outcomes leads to a nontrivial mixed state. The essential idea is to choose a unitary such that the two-point $Z_b Z_b$ operator evaluated in the mixed state amounts to the string operator $Z_b X_a \cdots X_a Z_b$ in the input SPT, thereby taking a nonzero expectation value.

First, for a postmeasurement pure state with outcome α, we apply a unitary U_α on B sublattice:

$$U_\alpha = \prod_i X_{b,i}^{\frac{1-\prod_{j=1,2,\ldots}^{i}\alpha_j}{2}}. \tag{4}$$

In other words, $X_{b,i}$, a Pauli X on B sublattice, is applied when there is an odd number of outcome -1 from the site $(a,1)$ to the site (a,i). It follows that $Z_{b,i}$ conjugated by U_α will acquire a 1 (-1) sign if there are even (odd) number of -1 measurement outcomes from the site $(a,1)$ to the site (a,i). Correspondingly, one finds $U_\alpha^\dagger Z_{b,i} Z_{b,j}\, U_\alpha = Z_{b,i}\left(\prod_{k=i+1}^{j}\alpha_k\right) Z_{b,j}$. The overall measurement and unitary operation lead to the mixed state $\rho = \sum_\alpha U_\alpha P_\alpha \rho_0 P_\alpha U_\alpha^\dagger$. The long-range order can be diagnosed by the two-point ZZ correlation on B sublattice:

$$\begin{aligned}
\mathrm{tr}[\rho Z_{b,i} Z_{b,j}] &= \sum_\alpha \langle\psi_0|\, P_\alpha U_\alpha^\dagger Z_{b,i} Z_{b,j}\, U_\alpha P_\alpha\, |\psi_0\rangle \\
&= \sum_\alpha \langle\psi_0|\, P_\alpha Z_{b,i}\left(\prod_{k=i+1}^{j}\alpha_k\right) Z_{b,j} P_\alpha\, |\psi_0\rangle \\
&= \langle\psi_0|\, Z_{b,i}\left(\prod_{k=i+1}^{j} X_{a,k}\right) Z_{b,j}\, |\psi_0\rangle,
\end{aligned} \tag{5}$$

where we have used the fact that the measurement outcome α_k can be replaced with $X_{a,k}$ due to the projector P_α, and $\sum_\alpha P_\alpha = 1$. Therefore, the two-point function in ρ is exactly the string order in the initial SPT order state, and hence $\langle Z_{b,i} Z_{b,j}\rangle = c = O(1) > 0$. As discussed in Sec. III, this nondecaying two-point function together with the $\mathbb{Z}_2$ symmetry on B sublattice, i.e., $\langle\prod_i X_{b,i}\rangle = 1$, indicates that $\rho_B (= \mathrm{tr}_A \rho)$ is a nontrivial mixed state with a GHZ-type quantum long-range order. Importantly, since the string order is a universal property of the input SPT, which is robust under any finite-time symmetry-preserving local unitary evolution, the convertibility to GHZ-type order is a universal property of the input SPT phase.

B. Duality transformation

As discussed in our general framework (Sec. II), our protocol can be viewed as realizing a controlled unitary $U = \sum_\alpha P_\alpha U_\alpha$ acting on the AB composite system followed by tracing out A. Specifically, starting from the input $|\psi_0\rangle$ with the Hamiltonian H_0, there exists a purification $|\psi\rangle$ of the output state $\rho_B (= \mathrm{tr}_A |\psi\rangle\langle\psi|)$ with $|\psi\rangle =$

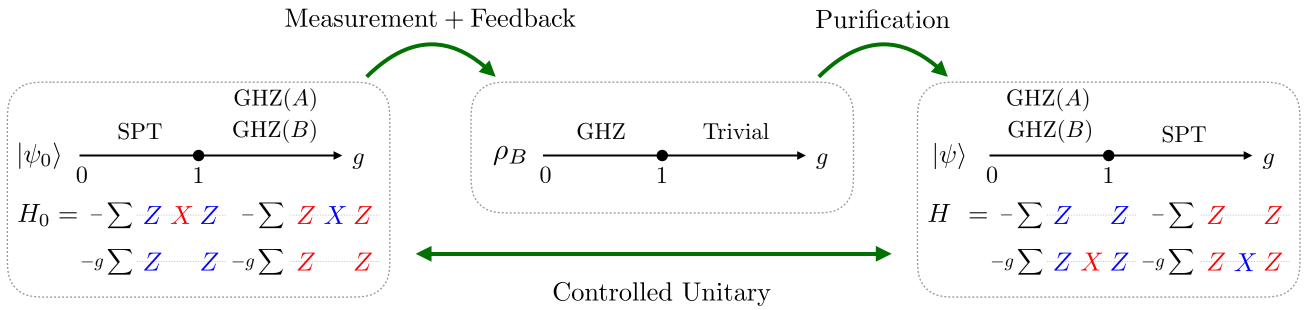

FIG. 2. Starting with an input $|\psi_0\rangle$, which undergoes a transition from a $\mathbb{Z}_2 \times \mathbb{Z}_2$ SPT order in the AB composite system to two independent GHZ-type symmetry breaking orders in A, B respectively, a measurement-feedback protocol leads to a density matrix on B (i.e., ρ_B), which undergoes a transition from a GHZ-type order to a trivial mixed state. ρ_B admits a purification $|\psi\rangle$ that can be obtained from the input state $|\psi_0\rangle$ via a controlled unitary $U = \sum_\alpha U_\alpha P_\alpha$, and the Hamiltonian of $|\psi\rangle$ can be derived based on the transformation rules [Eq. (6)]. The purification therefore provides a useful handle to characterize the structure of the output density matrix ρ_B.

$U|\psi_0\rangle$. This allows us to derive the parent Hamiltonian H of $|\psi\rangle$ through $H = UH_0U^\dagger$, so the structure of the output mixed state ρ_B can be characterized. Figure 2 provides a summary for this subsection.

With $U = \sum_\alpha P_\alpha U_\alpha$ [U_α defined in Eq. (4)], one derives the transformation rule for operators under the conjugation of U (see Appendix B 1 for details).

$$\begin{aligned} &X_{a,i} \to X_{a,i}, \quad X_{b,i} \to X_{b,i}, \\ &Z_{a,i}Z_{a,i+1} \to Z_{a,i}X_{b,i}Z_{a,i+1}, \\ &Z_{b,i}Z_{b,i+1} \to Z_{b,i}X_{a,i+1}Z_{b,i+1}. \end{aligned} \tag{6}$$

Pauli X is invariant since U is diagonal in X basis. On the other hand, neighboring ZZ on one sublattice is attached with a Pauli X on another sublattice in between two Pauli Zs. This is quite intuitive since the unitary feedback is designed to transform the product of two Pauli Zs on one sublattice with a sign that depends on the product of measurement outcomes (on another lattice) between these two Pauli Zs. We also note that the above duality mapping can be understood as implementing a Kramers-Wannier (KW) duality conjugated by a unitary U_{CZ} ($= \prod \mathrm{CZ}_{(a,i),(b,i)}\mathrm{CZ}_{(b,i),(a,i+1)}$) that prepares a $\mathbb{Z}_2 \times \mathbb{Z}_2$ cluster SPT [53]. This is dubbed twisted gauging in Ref. [54], which is in contrast to the gauging via Kramers-Wannier duality.

The above duality mapping provides a powerful tool to characterize the structure of the output mixed state; as an application, we consider the ground state of the following Hamiltonian as an input:

$$\begin{aligned} H_0 = &-\sum_i Z_{a,i}X_{b,i}Z_{a,i+1} - \sum_i Z_{b,i}X_{a,i+1}Z_{b,i+1} \\ &- g\sum_i Z_{a,i}Z_{a,i+1} - g\sum_i Z_{b,i}Z_{b,i+1}. \end{aligned} \tag{7}$$

The phase diagram of H_0 can be completely determined. To see this, by conjugating a product of controlled-Z gate: $U_{\mathrm{CZ}} = \prod \mathrm{CZ}_{(a,i),(b,i)}CZ_{(b,i),(a,i+1)}$, one obtains

$$\begin{aligned} &-\sum_i X_{b,i} - \sum_i X_{a,i} \\ &- g\sum_i Z_{a,i}Z_{a,i+1} - g\sum_i Z_{b,i}Z_{b,i+1}, \end{aligned} \tag{8}$$

i.e., two decoupled Ising chains on two sublattices, where $|g| < 1$ and $|g| > 1$ correspond to trivial phase and spontaneous symmetry breaking (SSB) phase with GHZ $\mathbb{Z}_2$ orders on A sublattice and B sublattice. This implies the ground state of H_0 belongs to SPT and SSB phase with GHZ order for $|g| < 1$ and $|g| > 1$, respectively.

Using the transformation rule in Eq. (6), one finds the measurement-feedback channel leads to a mixed state ρ_B on B sublattice, which is a reduced density matrix of the ground state $|\psi\rangle$ of the following Hamiltonian:

$$\begin{aligned} H = &-\sum_i Z_{a,i}Z_{a,i+1} - \sum_i Z_{b,i}Z_{b,i+1} \\ &- g\sum_i Z_{a,i}X_{b,i}Z_{a,i+1} - g\sum_i Z_{b,i}X_{a,i+1}Z_{b,i+1}. \end{aligned} \tag{9}$$

Comparing Eqs. (7) and (9), one finds they are dual to each other, and the phase of H can be determined analogously: A and B sublattices individually exhibit a GHZ order for $|g| < 1$, and the $A \bigcup B$ together exhibits SPT order for $|g| > 1$. Consequently, ρ_B possesses a mixed-state GHZ order for $|g| < 1$, and ρ_B becomes a trivial mixed state for $|g| > 1$ (since the subsystem of the SPT gives a trivial mixed state). In addition, since $|\psi\rangle$ can be obtained by applying extensive controlled-Z gates across A, B sublattices (i.e., $U_{\mathrm{CZ}} = \prod CZ_{(a,i),(b,i)}CZ_{(b,i),(a,i+1)}$) on two decoupled Ising chains on A/B sublattice, one expects $\rho_B = \mathrm{tr}_A |\psi\rangle\langle\psi|$ has volume-law entropy for any nonzero g (U_{CZ} acts trivially at $g = 0$). This is indeed the case based on our exact diagonalization calculation (see Appendix B 2).

While here we consider only one type of perturbation to illustrate the utility of the duality approach, in Appendix B 3 we discuss other types of perturbation, including independently tunable perturbation strength in $Z_{a,i}Z_{a,i+1}, Z_{b,i}Z_{b,i+1}$ as well as onsite Pauli-X perturbation. Interestingly, when perturbing the fixed-point SPT using onsite Pauli Xs, the corresponding output ρ_B is exactly the (pure) ground state of the transverse-field Ising chain in the symmetry-broken phase in the subspace with $\prod_i X_{b,i} = 1$.

C. Mixed-state quantum criticality

Our protocol can also output a mixed state with volume-law entropy coexisting with critical (algebraic) long-range order. This occurs when applying our measurement-feedback channel to a critical state, i.e., the ground state of H_0 in Eq. (7) at $g = 1$. In this case, the output will be a mixed state ρ_B on B sublattice by tracing out A sublattice for the ground state $|\psi\rangle$ of H in Eq. (9) at $g = 1$ [55], where $|\psi\rangle$ reads

$$|\psi\rangle = U_{\mathrm{CZ}} |\mathrm{CFT}\rangle_A \otimes |\mathrm{CFT}\rangle_B . \tag{10}$$

$|\mathrm{CFT}\rangle_{A/B}$ denotes the ground state of a transverse-field Ising chain (on A/B sublattice) at a critical point, characterized by the 1+1D Ising CFT, and $U_{\mathrm{CZ}} = \prod \mathrm{CZ}_{(a,i),(b,i)}\mathrm{CZ}_{(b,i),(a,i+1)}$. The corresponding mixed state $\rho_B = \mathrm{tr}_A |\psi\rangle\langle\psi|$ exhibits quantum criticality diagnosed by certain operators. For example, since U_{CZ} commutes with Pauli Zs, the two-point ZZ function is given by the single Ising critical chain, which exhibits an algebraic decay: $\langle Z_{b,i}Z_{b,j}\rangle = \langle\mathrm{CFT}|_B Z_{b,i}Z_{b,j} |\mathrm{CFT}_B\rangle \sim 1/|i-j|^\eta$ with $\eta = 1/4$ being a critical exponent in 1+1D Ising CFT. On the other hand, the disorder operator $X_{b,i}X_{b,i+1}\cdots X_{b,j}$ also exhibits an algebraic decay:

$$\begin{aligned}
&\langle X_{b,i}\cdots X_{b,j}\rangle \\
&= \langle\mathrm{CFT}|_A \langle\mathrm{CFT}|_B U^\dagger_{\mathrm{CZ}} X_{b,i}\cdots X_{b,j} U_{\mathrm{CZ}} |\mathrm{CFT}\rangle_A |\mathrm{CFT}\rangle_B \\
&= \langle\mathrm{CFT}|_A \langle\mathrm{CFT}|_B Z_{a,i}X_{b,i}\cdots X_{b,j} Z_{a,j+1} |\mathrm{CFT}\rangle_A |\mathrm{CFT}\rangle_B \\
&= \langle Z_{a,i}Z_{a,j+1}\rangle_{CFT,A} \langle X_{b,i}\cdots X_{b,j}\rangle_{CFT,B} \\
&\sim \frac{1}{|i-j|^{2\eta}},
\end{aligned} \tag{11}$$

where we used the Kramers-Wannier duality to convert $X_{b,i}X_{b,i+1}\cdots X_{b,j}$ to $Z_{b,i}Z_{b,j+1}$. Importantly, we note that the disorder operator is distinct from a single pure CFT, where $X_{b,i}X_{b,i+1}\cdots X_{b,j} \sim 1/|i-j|^\eta$.

The mixed state ρ_B exhibits genuine quantum criticality. Specifically, based on the two conditions, i.e., algebraic decay in ZZ two-point function and $\prod_i X_{b,i} = 1$, ρ_B cannot be an ensemble of short-range entangled pure states as discussed in Sec. III. To better characterize the entanglement signature for the mixed-state quantum criticality, we bipartition B sublattice into two intervals B_1 and B_2, and quantify their entanglement using entanglement negativity E_N [33–37], an entanglement measure of mixed states: $E_N(\rho_B) = \ln\left(||\rho_B^{T_{B_1}}||_1\right)$, where the upper script T_{B_1} denotes the partial transpose with respect to the subsystem B_1 and $||\cdot||_1$ denotes the trace norm. Using exact diagonalization (ED), we find (see Fig. 3) negativity follows a universal scaling form as in the 1+1D CFT [56,57]:

$$E_N(x, L) = \alpha \ln\left(\frac{L}{\pi}\sin\left(\frac{\pi x}{L}\right)\right) + \beta, \tag{12}$$

where x, L are the sizes of the subsystem B_1 and the entire B sublattice, and $\alpha \approx 0.15$. As a comparison, the finite-size numerics for a pure critical Ising chain reports $\alpha \approx 0.30$ [58]. This indicates that the amount of long-range entanglement on B sublattice decreases when coupling to A sublattice. Since the prefactor α is generically a universal number that relates to the number of low-energy degrees of freedom, one interpretation is that coupling between A, B sublattices diminishes the low-energy degrees of freedom that carry long-distance entanglement on B sublattice. This is also consistent with the fact that the disorder operator decays faster after coupling to A sublattice [Eq. (11)].

Finally, we remark that our protocol of converting hidden order is also applicable when the input state is mixed. One immediate application is that when the input pure SPT is subject to a symmetry-preserving noise channel, in which case the string order survives, the output of our measurement-feedback channel will remain long-range ordered. In addition, with the critical state [$g = 1$ in Eq. (7)] under a noise channel as an input, the output

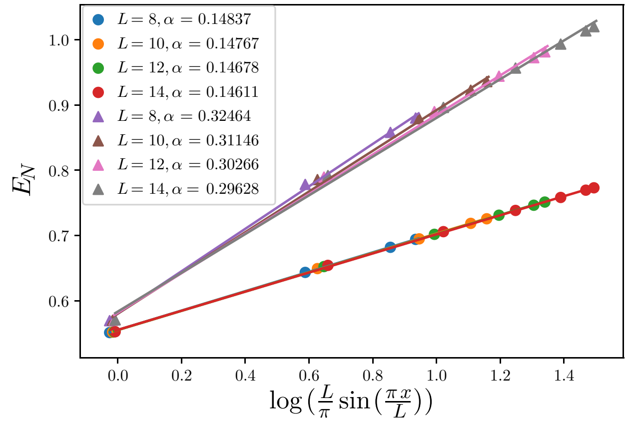

FIG. 3. Entanglement negativity E_N between two complementary segments of sizes x and $L - x$ on B sublattice. Data denoted by circles are for the critical mixed state resulting from measurement and feedback on the SPT critical point [equivalently, $\rho_B = \mathrm{tr}_A |\psi\rangle\langle\psi|$ with $|\psi\rangle$ defined in Eq. (10)]. The linear fit of the data indicates ρ_B has an entanglement structure like that of a 1+1D CFT. As a comparison, triangles correspond to the pure 1+1D Ising critical state $|\mathrm{CFT}\rangle_B$ on B.

mixed state exhibits a log scaling of bipartite entanglement negativity [as in Eq. (12)] while the log-scaling prefactor decreases continuously as increasing the noise rate. See Appendix B 4 for a detailed discussion.

D. Generalization to other mixed-state long-range order

Here we briefly summarize several classes of mixed-state long-range order that can be realized based on our general framework. In all these examples, we derive an exact duality between the Hamiltonian of the input SPT and the Hamiltonian of a purified state whose sublattice encodes the long-range order, which allows us to establish the correspondence between phase diagram of the input state and that of the output state.

$\mathbb{Z}_2$ **topological order in higher-space dimensions**: our protocol can be straightforwardly generalized by considering input states as $\mathbb{Z}_2$ p-form $\times\mathbb{Z}_2$ q-form SPTs in d-space dimension with $p+q=d-1$. Using measurement-feedback channels, one can prepare a mixed state with $\mathbb{Z}_2$ topological order at $d\geq 2$ space dimensions. In Appendix C we detail the realization of mixed-state $\mathbb{Z}_2$ topological order in 2d.

$\mathbb{Z}_2$ **fermionic topological order**: another straightforward application is the preparation of mixed states with $\mathbb{Z}_2$ fermionic topological order. This can be achieved by taking $\mathbb{Z}_2\times\mathbb{Z}_2^f$ SPTs [20,59–62] as input, where the first $\mathbb{Z}_2$ symmetry acts on qubits and the second $\mathbb{Z}_2^f$ is the parity symmetry on fermions. Based on certain nonlocal hidden orders in these SPTs, we devise a protocol that outputs fermionic mixed states with long-range order. In Appendix D we present the protocol that realizes the fermionic mixed state in 1D with the same long-range order as in the topological phase of the 1D Kitaev chain. In Appendix E we present the protocol that realizes the fermionic mixed states in 2D with intrinsic topological order.

V. MIXED-STATE QUANTUM CRITICALITY BY MEASURING FERMIONS

In this section, we construct quantum channels based on fermion occupation number measurement in spinful fermions. This is naturally motivated by Gutzwiller projection [63], a standard approach to construct exotic states of matter by projecting spinful noninteracting fermions into the subspace of single occupation number per lattice site, yielding a spin-1/2 wave function. For example, Gutzwiller projecting free fermions at half-filling in 1D leads to a critical ground state of the Haldane-Shastry model [64,65], a long-range interacting Heisenberg antiferromagnet with $1/r^2$ exchange coupling. In 2D, certain spin liquids with topological order can be constructed similarly (see Refs. [39,40] for reviews). More broadly, Gutzwiller projection may be viewed as an application of parton construction [66], a well-known approach to constructing nontrivial states by imposing certain constraints on noninteracting particles.

Gutzwiller projection and parton construction provides inspiration for using measurement to implement the projection. Indeed, Ref. [23] has presented a protocol to prepare the ground state of the Kitaev honeycomb model [67], where notably, the desired projection can be achieved by measuring fermions and applying a depth-1 local unitary feedback. However, beyond this specific model, starting with a generic state, postmeasurement states with unwanted measurement outcomes may not converge to the same target Gutzwiller projected state using finite-depth unitaries. This presents a difficulty in realizing Gutzwiller projection with measurement-based protocols. Here our framework avoids this conundrum. We will show that occupation-number measurement followed by appropriate unitary feedback enables the realization of nontrivial mixed states with certain long-distance quantum correlations. A field-theoretic understanding of the resulting mixed states and their correlations will be presented in forthcoming work [68].

A. Measuring 1D fermion

Taking 1D spinful free fermions as input, below we will present a finite-depth protocol for realizing quantum-critical mixed states with critical correlations distinct from the input states.

Consider noninteracting, spinful fermions on a 1D lattice, where the annihilation fermion operators at site i are denoted by $c_{i,s}, c_{i,s}^\dagger$ with site indices $i=1,2,\ldots,L$ and spin indices $s=\uparrow,\downarrow$, we define a tight-binding Hamiltonian $H=-\sum_{i,s}(c_{i+1,s}^\dagger c_{i,s}+\text{h.c.})$, whose ground state $|\psi_0\rangle$ takes the following form: $\prod_k c_{k,\uparrow}^\dagger \prod_k c_{k,\downarrow}^\dagger |0\rangle$ with k being the momentum indices. $|\psi_0\rangle$ exhibits an algebraic correlation between spins:

$$\left\langle S_i^z S_j^z\right\rangle \sim \frac{1}{(j-i)^2}, \tag{13}$$

with the spin operator $S_i^z=\frac{1}{2}[n_{i,\uparrow}-n_{i,\downarrow}]$, and $n_i=n_{i,\uparrow}+n_{i,\downarrow}$ is the number operator at site i.

Interestingly, by decorating with a fermion parity string, the spin-spin correlation decays slower (see Ref. [42] for details):

$$\left\langle S_i^z \prod_{l=i+1}^{j-1}(-1)^{n_l} S_j^z\right\rangle \sim \frac{1}{j-i}. \tag{14}$$

In other words, the fermion-parity string reveals a more ordered, long-range correlation that is hidden in free fermions. Conceptually the insertion of the fermion string has the effect of removing the charge fluctuations, thereby enhancing the order in the spin sector. The physics is akin to the spin-1 Affleck-Kennedy-Lieb-Tasaki (AKLT) chain [69] (belonging to the Haldane SPT phase [70]), where the ground state is a superposition of a class of product states that have a staggered pattern of $+1$ and -1 with an arbitrary number of 0s in between, e.g. $\cdots + 00 - 0 + 000 - + \cdots$. While the two-point function $S_i^z S_j^z$ decays exponentially due to the position disorder of 0, inserting the string $\prod_{l=i+1}^{j-1} (-1)^{S_l^z}$ in between S_i^z and S_j^z effectively removes the disorder, thereby revealing the hidden antiferromagnetic order [71]. The process of removing certain disorders by inserting string operators is dubbed the squeezed-space construction in Ref. [42].

More technically, the string order may be understood as the following: the free-fermion state consists of two decoupled fermion chains with opposite spin flavors: $|\psi_0\rangle = |\psi_0\rangle_\uparrow \otimes |\psi_0\rangle_\downarrow$. Each fermion chain exhibits a string order $c_{i,s}^\dagger \prod_{l=i+1}^{j-1} (-1)^{n_{l,s}} c_{j,s} \sim 1/\sqrt{|j-i|}$ with $s \in \{\uparrow, \downarrow\}$ [72]. Considering a product of two string operators, one finds $S_i^\dagger \prod_{l=i+1}^{j-1} (-1)^{n_l} S_j^- \sim 1/j - i$, where $S_i^\pm$ is the spin raising and lowering operator. Using the spin rotational symmetry, one then recovers the string order in Eq. (14).

Given the above free-fermion state $|\psi_0\rangle$, measuring the fermion occupation number at each site gives the outcome $n = \{n_1, n_2, \dots, n_L\}$ with each $n_i \in \{0, 1, 2\}$. Correspondingly, the postmeasurement state becomes $P_n |\psi_0\rangle / \sqrt{\langle\psi_0| P_n |\psi_0\rangle}$ with probability $p_n = \langle\psi_0| P_n |\psi_0\rangle$. The measurement-only protocol leads to a mixed state $\rho_m = \sum_n P_n \rho_0 P_n$, i.e., an ensemble of pure states corresponding to distinct measurement outcomes. Since spin operators commute with fermion number operators, the spin-spin correlation remains unchanged: $\mathrm{tr}\left[\rho_m S_i^z S_j^z\right] = \langle\psi_0| S_i^z S_j^z |\psi_0\rangle \sim 1/(j-i)^2$.

Now we show that with appropriate unitary feedback, one can obtain a mixed state with enhanced long-range correlation. Specifically, the string order of the original input state $|\psi_0\rangle$ will be transformed into spin-spin correlation with $S_i^z S_j^z \sim 1/j - i$ in the resulting mixed state. This is in strong contrast to $S_i^z S_j^z \sim 1/(j-i)^2$ in the case without unitary feedback.

The protocol is as follows. First, we measure the fermion occupation number on every site. For each postmeasurement state with an outcome labeled by n, we apply a local unitary U_n. This depth-2 protocol leads to a mixed state: $\rho = \sum_n U_n P_n \rho_0 P_n U_n^\dagger$. Now we look for the unitary U_n that transforms S_i^z to $S_i^z (-1)^{\sum_{j \le i} n_j}$ for all i. This can be achieved by choosing

$$U_n = \prod_{i=1}^{L} \left(\mathcal{S}_i^x\right)^{\sum_{j \le i} n_j}, \tag{15}$$

where $\mathcal{S}_i^x$ is a spin-flip operator: $\mathcal{S}_i^x = 2S_i^x = c_{i,\uparrow}^\dagger c_{i,\downarrow} + c_{i,\downarrow}^\dagger c_{i,\uparrow}$ in the subspace of $n_i = 1$, and $\mathcal{S}_i^x = 1$ (i.e., it acts trivially) in the subspace of $n_i = 0, 2$. In other words, the operator $\mathcal{S}_i^x$ is applied at site i when there is an odd number of fermions in the interval $[1, i]$.

Under the transformation by U_n, the spin-spin correlator becomes $U_n^\dagger S_i^z S_j^z U_n = -S_i^z (-1)^{\sum_{l=i+1}^{j-1} n_l} S_j^z$, which acquires a sign that depends on the number of fermions between sites i and j. A straightforward calculation shows that

$$\begin{aligned} \mathrm{tr}\left[\rho S_i^z S_j^z\right] &= \sum_n \langle\psi_0| P_n U_n^\dagger S_i^z S_j^z U_n P_n |\psi_0\rangle \\ &= -\langle\psi_0| S_i^z (-1)^{\sum_{l=i+1}^{j-1} n_j} S_j^z |\psi_0\rangle \\ &\sim \frac{1}{j-i}. \end{aligned} \tag{16}$$

Therefore, the hidden string order of the input state $|\psi_0\rangle$ is converted to a critical correlation shared among spins in the output mixed state ρ. In particular, the reduced density matrix of ρ that describes spins, obtained by tracing out charge fluctuations, can be purified into a ground state of a local Hamiltonian that describes *interacting* spinful fermions (see Appendix F).

One may also consider the spin-spin correlation in other orientations. The global SU(2) spin-rotation symmetry of the input state $|\psi_0\rangle$ implies $\langle\psi_0| S_i^\nu S_j^\nu |\psi_0\rangle \sim 1/(j-i)^2$ and $\langle\psi_0| S_i^\nu \prod_{l=i+1}^{j-1} (-1)^{n_l} S_j^\nu |\psi_0\rangle \sim 1/(j-i)$ for $\nu = x, y, z$. Since the feedback unitary consists of $\mathcal{S}_i^x$, which anticommutes with S_i^y, the channel also boosts the correlation in y component, i.e., $S_i^y S_j^y$ is enhanced from $1/(j-i)^2$ to $(1/j - i)$ in the resulting mixed state. On the other hand, correlation in x component remains $1/(j-i)^2$ since the spin operator in x component transforms trivially under the unitary feedback.

The mixed state arising from our protocol is nontrivial in the sense that it cannot be written as a mixture of short-range entangled states. To see this, we first note that due to the global spin-flip symmetry of the input state, i.e., $\prod_i \mathcal{S}_i^x |\psi_0\rangle = |\psi_0\rangle$, the output mixed state ρ will have $\prod_i \mathcal{S}_i^x = 1$ in the expectation value as well (since this operator commutes with both measurement operators and unitary correction). Based on the algebraic decay $S_i^z S_j^z$ and $\prod_i \mathcal{S}_i^x = 1$, one can again use the proof technique in Sec. III to show that ρ cannot be a mixture of short-range entangled states. This, in turn, suggests certain long-distance entanglement in the mixed state. Specifically, in light of the well-known $\log L$ entanglement scaling of the input free fermions in 1D, the output state will likely exhibit a $\log L$ scaling mixed-state entanglement (e.g., quantified by entanglement negativity).

When considering interactions in the input state, our protocol continues to generate critical mixed states. As shown in Ref. [42], given interacting fermions described by a Luttinger liquid with the Luttinger parameters K_s and K_c corresponding to the stiffness of spins and charges, with repulsive charge interaction (implying $0 < K_c < 1$) and global SU(2) spin-rotation symmetry (implying $K_s = 1$), the leading-order spin-spin correlation behaves as $S_i^z S_j^z \sim 1/(j-i)^{K_c+K_s}$ and the string operator behaves as $S_i^z \prod_{l=i+1}^{j-1}(-1)^{n_l} S_j^z \sim 1/(j-i)^{K_s}$. Using the same measurement-feedback channel, one can then transform this string order to a critical spin-spin correlation $S_i^z S_j^z \sim 1/(j-i)^{K_s}$ in the resulting mixed state, which is in contrast to the initial exponent $K_c + K_s$.

B. Measuring Chern insulators

Here, we show that starting with a two-dimensional gapped state with short-range correlations in the bulk, measurement and feedback can remarkably lead to a mixed state with long-range *critical* correlations.

Our starting point is the Chern insulator, a gapped state of matter, which features integer-value quantized Hall conductance and gapless edge states. Despite the short-range correlation in the bulk, i.e., exponential decay of two-point functions, there exists a nonlocal operator whose correlation decays algebraically. Denoting a fermion creation operator by $c^\dagger(\mathbf{x})$ with $\mathbf{x} = (x, y)$ being the space coordinate, one defines a dressed fermion creation operator $\tilde{c}^\dagger(\mathbf{x}) = \eta(\mathbf{x}) c^\dagger(\mathbf{x})$, where $\eta(\mathbf{x})$ is a nonlocal operator:

$$\eta(\mathbf{x}) = e^{i\int d^2x' c^\dagger(\mathbf{x}')c(\mathbf{x}')\arg(\mathbf{x}-\mathbf{x}')}, \tag{17}$$

with $\arg(\mathbf{x})$ being the polar angle of $\mathbf{x}$.

In a Chern insulator $|\nu = 1\rangle$ with associated Hall conductance $\sigma_H = \nu(e^2/h)$, the dressed operators exhibit a critical correlation [45]:

$$\langle \nu = 1| \tilde{c}(\mathbf{x})\tilde{c}^\dagger(\mathbf{x}') |\nu = 1\rangle \sim \frac{1}{|\mathbf{x}-\mathbf{x}'|^\alpha}, \tag{18}$$

where α is a nonuniversal constant related to the $U(1)$ response of Chern insulators.

As discussed in Ref. [45], $\eta(\mathbf{x})$ can be understood as the operator associated with the infinitesimal time evolution given by inserting a 2+1D $U(1)$ monopole, and the algebraic long-range order results from the topological response to such monopole insertion in a Chern insulator. Note that the above critical order presents an off-diagonal long-range order (ODLRO), which was first discovered by Girvin and MacDonald [44] in fractional quantum Hall states at filling fraction $\nu = 1/m$. In particular, these quantum Hall states may be understood as a condensate of composite bosons by attaching fluxes to fermions, so the bare fermions need to be dressed by an appropriate nonlocal operator Eq. (17) in order to reveal the hidden ODLRO. For quantum Hall states described by Laughlin's wave function at $\nu = 1$, α is analytically found to be 1/2 [44].

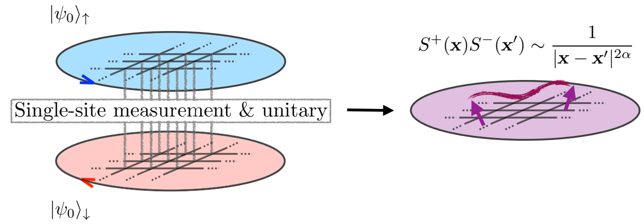

FIG. 4. Spin-up and spin-down fermions are initialized in Chern insulating states with opposite Chern numbers. Such an initial state can be converted to a mixed state with algebraic correlations in the bulk through a two-step protocol consisting of single-site fermion occupation-number measurement and unitary.

Below we will discuss a protocol that realizes a critical mixed state with algebraic two-point correlations based on the hidden order in Chern insulators (see Fig. 4). To start, we consider an initial state $|\psi_0\rangle = |\psi_0\rangle_\uparrow \otimes |\psi_0\rangle_\downarrow$, where $|\psi_0\rangle_\uparrow$ is the Chern insulator with $\nu = 1$ consisting of spin-up fermions, and $|\psi_0\rangle_\downarrow$ is the Chern insulator with $\nu = -1$ consisting of spin-down fermions. As a result, spin-up and spin-down fermions, respectively, exhibit an algebraic hidden order:

$$\langle\psi_0|_s \tilde{c}_s(\mathbf{x})\tilde{c}_s^\dagger(\mathbf{x}') |\psi_0\rangle_s \sim \frac{1}{|\mathbf{x}-\mathbf{x}'|^\alpha}, \tag{19}$$

where $s = 1, -1$ for spin-up and spin-down fermions, and the dressed fermion operators are $\tilde{c}_s^\dagger(\mathbf{x}) = \eta_s(\mathbf{x}) c_s^\dagger(\mathbf{x})$, with

$$\eta_s(\mathbf{x}) = e^{is\int d^2x' c_s^\dagger(\mathbf{x}')c_s(\mathbf{x}')\arg(\mathbf{x}-\mathbf{x}')}. \tag{20}$$

Note the opposite sign in the exponent is due to the opposite sign of Chern numbers for spin-up and spin-down fermions.

The hidden critical order in the Chern insulators can be detected through spin-raising and lowering operators $S^+(\mathbf{x}) = c_\uparrow^\dagger(\mathbf{x})c_\downarrow(\mathbf{x})$ and $S^-(\mathbf{x}) = c_\downarrow^\dagger(\mathbf{x})c_\uparrow(\mathbf{x})$ by dressing them with the appropriate nonlocal operators. Specifically, let $\hat{n}_\uparrow(\mathbf{x}), \hat{n}_\downarrow(\mathbf{x})$ be the number operator of spin-up and -down fermions, and define $\hat{\phi}(\mathbf{x}) = \int d^2x' \hat{n}(\mathbf{x})\arg(\mathbf{x}-\mathbf{x}')$ with $\hat{n}(\mathbf{x}) = \hat{n}_\uparrow(\mathbf{x}) + \hat{n}_\downarrow(\mathbf{x})$. Then the nonlocal operator $e^{i\hat{\phi}(\mathbf{x})}S^+(\mathbf{x})S^-(\mathbf{x}')e^{-i\hat{\phi}(\mathbf{x}')}$ exhibits an algebraic decay:

$$\begin{aligned}
&\langle\psi_0| e^{i\hat{\phi}(\mathbf{x})}S^+(\mathbf{x})S^-(\mathbf{x}')e^{-i\hat{\phi}(\mathbf{x}')} |\psi_0\rangle \\
&= \langle\psi_0| \tilde{c}_\uparrow^\dagger(\mathbf{x})\tilde{c}_\downarrow(\mathbf{x})\tilde{c}_\downarrow^\dagger(\mathbf{x}')\tilde{c}_\uparrow(\mathbf{x}') |\psi_0\rangle \\
&= -\langle\psi_0|_\uparrow \tilde{c}_\uparrow(\mathbf{x}')\tilde{c}_\uparrow^\dagger(\mathbf{x}) |\psi_0\rangle_\uparrow \langle\psi_0|_\downarrow \tilde{c}_\downarrow(\mathbf{x})\tilde{c}_\downarrow^\dagger(\mathbf{x}') |\psi_0\rangle_\downarrow \\
&\sim \frac{1}{|\mathbf{x}-\mathbf{x}'|^{2\alpha}}.
\end{aligned} \tag{21}$$

Now we show how to convert this hidden nonlocal order to a critical order in the two-point function $S^+(\mathbf{x})S^-(\mathbf{x}')$

using measurement and feedback. In particular, since the nonlocal order in the input state is a universal property of the Chern insulator phase, our protocol will always give rise to a state with critical correlations as long as the input state is in the same phase of matter. Starting with the input state $|\psi_0\rangle$, we measure the fermion occupation number on every site and then provide unitary feedback. The resulting density matrix takes the form:

$$\rho = \sum_n U_n P_n |\psi_0\rangle \langle\psi_0| P_n U_n^\dagger, \tag{22}$$

where P_n is the projector to a definite fermion number configuration, and U_n is the unitary feedback

$$U_n = \prod_{\mathbf{x}} e^{-i\phi_n(\mathbf{x})S^z(\mathbf{x})} \tag{23}$$

with $S^z(\mathbf{x}) = \frac{1}{2}(\hat{n}_\uparrow(\mathbf{x}) - \hat{n}_\downarrow(\mathbf{x}))$ and the phase $\phi_n(\mathbf{x}) = \int d^2x' n(\mathbf{x})\arg(\mathbf{x}-\mathbf{x}')$ depending on the measurement outcome. The resulting density matrix ρ exhibits a critical two-point correlation inherited from the nonlocal hidden order of the input $|\psi_0\rangle$:

$$\begin{aligned}&\mathrm{tr}\left[\rho S^+(\mathbf{x})S^-(\mathbf{x}')\right]\\ &\quad= \langle\psi_0| e^{i\hat{\phi}(\mathbf{x})} S^+(\mathbf{x})S^-(\mathbf{x}') e^{-i\hat{\phi}(\mathbf{x}')} |\psi_0\rangle \sim \frac{1}{|\mathbf{x}-\mathbf{x}'|^{2\alpha}}.\end{aligned} \tag{24}$$

To see this, one first notes that the spin operators under the transformation by U_n will be dressed by an appropriate phase, namely,

$$\begin{aligned}U_n^\dagger S^+(\mathbf{x}) U_n &= e^{i\phi_n(\mathbf{x})} S^+(\mathbf{x}),\\ U_n^\dagger S^-(\mathbf{x}) U_n &= e^{-i\phi_n(\mathbf{x})} S^-(\mathbf{x}).\end{aligned} \tag{25}$$

This implies $P_n U_n^\dagger S^+(\mathbf{x})S^-(\mathbf{x}')U_n P_n = P_n e^{i\hat{\phi}(\mathbf{x})} S^+(\mathbf{x}) S^-(\mathbf{x}') e^{-i\hat{\phi}(\mathbf{x}')}$, where the phase $\phi_n(\mathbf{x})$ has been promoted to an operator $\hat{\phi}(\mathbf{x})$ under the projector P_n. Using this result, it is then straightforward to derive Eq. (24) with the density matrix in Eq. (22).

Similarly, one may compute $S^-(\mathbf{x})S^+(\mathbf{x}')$, which turns out to be equal to $S^+(\mathbf{x})S^-(\mathbf{x}')$ in the operator expectation value, hence decaying algebraically. These two results together imply $S_x(\mathbf{x})S_x(\mathbf{x}') + S_y(\mathbf{x})S_y(\mathbf{x}') = \frac{1}{2}(S^+(\mathbf{x})S^-(\mathbf{x}') + S^-(\mathbf{x})S^+(\mathbf{x}')) \sim 1/|\mathbf{x}-\mathbf{x}'|^{2\alpha}$, where $S_x(\mathbf{x}) = \frac{1}{2}(S^+(\mathbf{x}) + S^-(\mathbf{x})), S_y(\mathbf{x}) = (S^+(\mathbf{x}) - S^-(\mathbf{x}))/(2i)$, i.e., the spin operator in x and y component. In particular, since the initial input state $|\psi_0\rangle$ satisfies $\prod_{\mathbf{x}} \mathcal{S}^z(\mathbf{x})|\psi_0\rangle = |\psi_0\rangle$, where $\mathcal{S}^z(\mathbf{x})$ is the π rotation about z axis, the expectation value of $\mathcal{S}^z(\mathbf{x})$ is one in the resulting mixed state. With the proof technique used in Sec. III, $\mathcal{S}^z(\mathbf{x}) = 1$ together with algebraic decay of $S_x(\mathbf{x})S_x(\mathbf{x}') + S_y(\mathbf{x})S_y(\mathbf{x}')$ indicate that the critical mixed state ρ cannot be a mixture of short-range entangled state.

VI. SUMMARY AND DISCUSSION

In this work, we present a general framework for realizing mixed-state quantum order and quantum criticality using finite-depth quantum channels consisting of local measurement, local unitary feedback, and nonlocal classical communication. As an illustration, our protocol universally converts certain SPT phases to mixed states with long-range (topological) orders. In addition, when the input SPT is tuned to a critical point, our protocol outputs a quantum critical mixed state diagnosed by volume-law classical entropy, algebraic decay of correlations, as well as logarithmically scaling bipartite mixed-state entanglement. Within the same theoretical framework, we also show how to transform the correlation exponent in constant depth by considering 1D spinful free fermions. More interestingly, our protocol can convert Chern insulators to a mixed state with an algebraically decaying correlation in the bulk. This furnishes a notable example where mixed-state quantum criticality can emerge from gapped states of matter in finite depth.

Our work motivates several questions that are worth further exploration. First, while we provide several examples of realizing nontrivial mixed states with critical correlations, a deeper understanding of the entanglement structure of these novel mixed-state quantum criticality is lacking. Second, since this work focuses only on the utility of depth-2 protocols with onsite measurement and onsite unitary feedback, it would be interesting to generalize the current protocol, which may enable the realization of more types of exotic mixed-state orders and criticality. For instance, the onsite unitary feedback may be generalized to finite-depth local unitary circuits, and the current depth-2 protocols may be extended to multiple rounds of measurement and unitary layers.

Finally, it remains unclear what are the limitations of local measurement, local unitary, and nonlocal classical communication for realizing nontrivial quantum orders and criticality. Answering this question would provide sharp distinctions between the states that can and cannot be realized in finite depth. While entanglement provides one such constraint as discussed in Sec. III, it would be desirable to explore the limitations from various aspects in the future (see Refs. [25,73] for progress along this direction).

ACKNOWLEDGMENTS

The authors thank the Kavli Institute for Theoretical Physics (KITP), where this research was initiated and partly performed. The K.I.T.P. is supported, in part, by the National Science Foundation under Grant No. NSF PHY-1748958. S.V. and Z.Z. thank Matthew Fisher, Ali Lavasani, Andreas Ludwig, and Cenke Xu for helpful discussions. S.V. also acknowledges the support of the W. M. Keck Foundation (Grant No. 9303). T.-C.L. and T.H. thank Tarun Grover, Shengqi Sang, Liujun Zou, and Yijian

Zou for helpful discussions. T.-C.L. and T.H.'s research at Perimeter Institute is supported in part by the Government of Canada through the Department of Innovation, Science and Economic Development Canada and by the Province of Ontario through the Ministry of Colleges and Universities.

APPENDIX A: CONSTRAINTS ON MIXED-STATE ENTANGLEMENT

Here we first review the basic notion of entanglement of formation, which we will use to constrain the entanglement structure of output states from finite-depth quantum channels.

Entanglement of formation: given a density matrix $\rho_{C\overline{C}}$ acting on the bipartite Hilbert space $\mathcal{H}_C \otimes \mathcal{H}_{\overline{C}}$, the entanglement between C and $\overline{C}$ can be quantified via entanglement of formation E_f [46], which is defined as follows: one may decompose a density matrix into a convex sum of pure states, i.e., $\rho_{C\overline{C}} = \sum_i p_i |\psi_i\rangle\langle\psi_i|$ with $p_i \geq 0$ and $\sum_i p_i = 1$. Then $E_f \equiv \text{Min}\left\{\sum_i p_i S_C(\text{tr}_{\overline{C}} |\psi_i\rangle\langle\psi_i|)\right\}$, where $S_C(\rho_C)$ is the von Neumann entropy of ρ_C. Namely, E_f is the average of bipartite entanglement entropy minimized over all possible ways of decomposing ρ as a mixture of pure states. When $\rho_{C\overline{C}}$ is pure, E_f reduces to the von Neumann entanglement entropy. To demonstrate the idea of entanglement of formation, one may consider two qubits in a maximally mixed state, i.e., $\rho = \mathbb{I}/4$ with $\mathbb{I}$ being the identity operator. Certainly, the mixed state canbe written as a uniform mixture of four Bell states $(|00\rangle \pm |11\rangle)/\sqrt{2}, (|01\rangle \pm |10\rangle)/\sqrt{2}$, so the average entanglement is $\log 2$. However, the mixed state can also be written as a uniform mixture of four product states, $|00\rangle, |01\rangle, |10\rangle, |11\rangle$, in which case one achieves the minimal average entanglement entropy, i.e., zero. Therefore, $E_f = 0$ for this maximally mixed state.

Bounds on entanglement: in the main text, we construct quantum channels from LOCC, i.e., single-site measurement, single-site unitaries, and classical communication. As such, the mixed-state entanglement quantified by E_f must be nonincreasing under such quantum channels. To see this, starting with a state $\rho_0 = |\psi_0\rangle\langle\psi_0|$, performing single-site measurement followed by single-site unitaries leads to a mixed state ρ, a mixture of pure states $|\psi_\alpha\rangle = U_\alpha P_\alpha |\psi_0\rangle / \sqrt{\langle\psi_0| P_\alpha |\psi_0\rangle}$ with corresponding probability $p_\alpha = \langle\psi_0| P_\alpha |\psi\rangle$. Being an entanglement measure, E_f cannot increase on average under LOCC [46,74], indicating $E_f(\rho_0) \geq \sum_\alpha p_\alpha E_f(|\psi_\alpha\rangle) = \sum_\alpha p_\alpha S_C(\text{tr}_{\overline{C}} |\psi_\alpha\rangle\langle\psi_\alpha|)$. Meanwhile, one has $\sum_\alpha p_\alpha S_C(\text{tr}_{\overline{C}} |\psi_\alpha\rangle\langle\psi_\alpha|) \geq E_f(\rho = \sum_\alpha p_\alpha |\psi_\alpha\rangle\langle\psi_\alpha|)$ because E_f is the average entanglement entropy minimized over all possible pure state realizations. As a result, one finds $E_f(\rho_0) \geq E_f(\rho)$.

When generalizing onsite unitary operations to multisite, geometrically local unitary gates, the protocol no longer belongs to LOCC, and mixed-state entanglement may increase. To bound the entanglement growth, one may consider the Renyi-n entanglement of formation [75] defined as $R_n \equiv \text{Min}\left\{\sum_i p_i S_C^{(n)}(\text{tr}_{\overline{C}} |\psi_i\rangle\langle\psi_i|)\right\}$, where $S_C^{(n)}$ is the Renyi-n entropy. Starting with a pure state, after a finite-depth protocol with local measurement and unitary gates (acting on $O(1)$ number of neighboring sites), one obtains an ensemble ρ of pure-state trajectories $|\psi_\alpha\rangle$ with probability p_α. For each pure-state trajectory $|\psi_\alpha\rangle$, the increase of Renyi-0 entanglement $S_C^{(0)}(\text{tr}_{\overline{C}} |\psi_\alpha\rangle\langle\psi_\alpha|)$, also dubbed max entropy or Hartley entropy, is upper bounded by $D|\partial A|$, where D is the depth of the channel and $|\partial A|$ is the bipartition boundary area. This is because Hartley entropy is simply bounded by the number of local measurements and unitary gates that act on the boundary. Therefore, the increase of Renyi-0 entanglement of formation R_0 is also bounded by the area law. One immediate consequence is that if one starts with a pure product state (i.e., with $R_0 = 0$), then after a finite-depth channel, the Renyi entanglement of formation of any Renyi index will follow an area law since $R_n \leq R_0$ for any $n > 0$.

APPENDIX B: MEASURING 1D SPT

1. Derivation of operator duality

Here we derive the transformation rules for operators under the controlled unitary $U = \sum_\alpha P_\alpha U_\alpha$. U_α is the unitary feedback defined as $U_\alpha = \prod_i X_{b,i}^{(1-\prod_{j=1,2,\ldots}^{i} \alpha_j)/2}$. P_α is a projector defined as $P_\alpha = |\alpha\rangle\langle\alpha|$, which projects A sublattice to a product state in Pauli-X basis. Below we provide two distinct approaches for derivation.

Operator-based approach: first, the controlled unitary can be written as $U = \prod_i X_{b,i}^{(1-\prod_{j=1}^{i} X_{a,j})/2}$. Since U is diagonal in the Pauli-X basis, Pauli-X operators are invariant under the conjugation by U. Next, we consider $UZ_{b,i}Z_{b,i+1}U^\dagger$ (note that Pauli Zs come in pairs due to the global $\mathbb{Z}_2$ symmetry). This operator can be simplified as $uZ_{b,i}Z_{b,i+1}u^\dagger$, where

$$u = X_{b,i}^{\frac{1-\prod_{j=1}^{i} X_{a,j}}{2}} X_{b,i+1}^{\frac{1-\prod_{j=1}^{i+1} X_{a,j}}{2}}. \tag{B1}$$

In the subspace that $\prod_{j=1}^{i} X_{a,j} = 1$, one finds $UZ_{b,i}Z_{b,i+1} U^\dagger = X_{b,i+1}^{(1-X_{a,i+1})/2} Z_{b,i}Z_{b,i+1} X_{b,i+1}^{(1-X_{a,i+1})/2}$. For $X_{a,i+1} = 1$, one has $UZ_{b,i}Z_{b,i+1}U^\dagger = Z_{b,i}Z_{b,i+1}$ while for $X_{a,i+1} = -1$ one has $UZ_{b,i}Z_{b,i+1}U^\dagger = -Z_{b,i}Z_{b,i+1}$. Combining the cases of $X_{a,i+1} = \pm 1$ leads to the result $UZ_{b,i}Z_{b,i+1}U^\dagger = Z_{b,i}X_{a,i+1}Z_{b,i+1}$. Similarly, one finds $UZ_{a,i}Z_{a,i+1}U^\dagger = Z_{a,i}X_{b,i}Z_{a,i+1}$.

Here we remark that as we see in the main text, the controlled unitary $U = \prod_i X_{b,i}^{(1-\prod_{j=1}^{i} X_{a,j})/2}$ maps a $\mathbb{Z}_2 \times \mathbb{Z}_2$ SPT to two $\mathbb{Z}_2$ symmetry-breaking (GHZ) ordered states on A and B sublattices. This is akin to the Kennedy-Tasaki transformation [76,77], which transforms a Haldane spin-1 chain [70] with $\mathbb{Z}_2 \times \mathbb{Z}_2$ SPT order to two spontaneous $\mathbb{Z}_2$ symmetry-breaking orders. Indeed, Kennedy-Tasaki transformation can also be realized as a controlled unitary [78], which therefore fits into our general framework. In particular, we can take a Haldane spin-1 chain in the $\mathbb{Z}_2 \times \mathbb{Z}_2$ SPT phase, and perform a layer of onsite measurement followed by a layer of onsite unitaries to realize a mixed state with $\mathbb{Z}_2$ GHZ-like order.

Wave-function based approach: starting with a global $\mathbb{Z}_2 \times \mathbb{Z}_2$ symmetric input state $|\psi_0\rangle$, in Pauli-X basis $|\psi_0\rangle$ can be written as

$$|\psi_0\rangle = \sum_{\alpha,\beta}{}^{'} (-1)^{\chi(\alpha,\beta)} \psi(\alpha,\beta)\, |\alpha,\beta\rangle\,. \tag{B2}$$

$\alpha = \{\alpha_i = \pm 1\}, \beta = \{\beta_i = \pm 1\}$ denote the product state in Pauli-X basis in the sublattice A and sublattice B. The $\mathbb{Z}_2$ symmetry on each sublattice implies that the allowed α, β must satisfy $\prod_i \alpha_i = \prod_i \beta_i = 1$. We use Σ' to denote that only those α, β that satisfy this constraint are considered.

Due to the symmetry, $\alpha_i = -1$ must come in pairs, which can be regarded as the two endpoints of a string. Correspondingly, various α configurations can be understood as various A strings in A sublattice, and similarly, β configurations can be represented by B strings in B sublattice. Within the string representations, χ is the number of times that A strings intersect (braid) with B strings. When $|\psi_0\rangle$ is a fixed-point cluster SPT with ZXZ stabilizers, $\psi(\alpha,\beta)$ is a constant independent of α, β (see Fig. 5).

Given Eq. (B2), measuring Pauli X on A sublattice projects A sublattice to a particular α configuration: $P_\alpha |\psi_0\rangle = |\alpha\rangle \otimes \sum'_\beta (-1)^{\chi(\alpha,\beta)} \psi(\alpha,\beta)\, |\beta\rangle$. After

$$|\psi_0\rangle = \sum_{\alpha,\beta}{}^{'} (-1)^{\chi(\alpha,\beta)} |\alpha,\beta\rangle$$

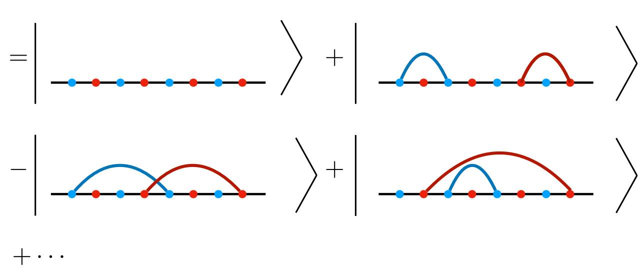

FIG. 5. 1D fixed-point $\mathbb{Z}_2 \times \mathbb{Z}_2$ SPT (with parent Hamiltonian $H_0 = -\sum_i Z_{a,i} X_{b,i} Z_{a,i+1} - \sum_i Z_{b,i} X_{a,i+1} Z_{b,i+1}$) as a condensate of two types of strings with a braiding sign structure in the Pauli-X basis. A product state $|\alpha,\beta\rangle$ in X basis with $\prod_i \alpha_i = \prod_i \beta = 1$ corresponds to a configuration of blue strings and red strings whose endpoints indicate $\alpha_i = -1$ and $\beta_i = -1$, respectively. The braiding number $\chi(\alpha,\beta)$ counts the number of times that two types of strings intersect.

the measurement, applying the unitary feedback $U_\alpha (= \prod_i X_{b,i}^{(1-\prod_{j=1,2,\ldots}^{i} \alpha_j)/2})$ removes the braiding phase: $U_\alpha P_\alpha |\psi_0\rangle = |\alpha\rangle \otimes \sum'_\beta \psi(\alpha,\beta)\, |\beta\rangle$. It follows that the output state on B sublattice reads

$$\begin{aligned}\rho_B &= \mathrm{tr}_A \left(\sum_\alpha U_\alpha P_\alpha |\psi_0\rangle \langle\psi_0| P_\alpha U_\alpha^\dagger \right) \\ &= \sum_{\beta,\beta'}{}^{'} |\beta\rangle\langle\beta'| \sum_\alpha{}^{'} \psi(\alpha,\beta)\psi^*(\alpha,\beta').\end{aligned} \tag{B3}$$

ρ_B is simply the reduced density matrix on B of the following pure state:

$$|\psi\rangle = \sum_{\alpha,\beta}{}^{'} \psi(\alpha,\beta)\, |\alpha,\beta\rangle\,. \tag{B4}$$

One consequence is that the entropy of the mixed state ρ_B results from the entanglement entropy between A and B in $|\psi\rangle$, i.e., it is the residual quantum fluctuation when removing the braiding phase in the initial input SPT $|\psi_0\rangle$.

Comparing Eqs. (B2) and (B4), it is obvious that $|\psi\rangle = U|\psi_0\rangle$ with U is a diagonal matrix whose entries encode the braiding phase:

$$U = \sum_{\alpha,\beta}{}^{'} |\alpha,\beta\rangle\langle\alpha,\beta|\, (-1)^{\chi(\alpha,\beta)}. \tag{B5}$$

Although U is not unitary in the entire Hilbert space, it is unitary in the symmetric subspace specified by $\prod_i X_{a,i} = \prod_i X_{b,i} = 1$. Note that this form of unitary has appeared in the literature [79] as a way to reveal the hidden long-range order of certain SPTs. We also note that in the symmetric subspace, U is the same as the controlled unitary $\sum_\alpha P_\alpha U_\alpha = \prod_i X_{b,i}^{(1-\prod_{j=1}^{i} X_{a,j})/2}$ discussed in the operator-based approach.

With $U = \sum'_{\alpha,\beta} (-1)^{\chi(\alpha,\beta)} |\alpha,\beta\rangle\langle\alpha,\beta|$, one can derive the parent Hamiltonian of $|\psi\rangle$ from $H = U H_0 U^\dagger$, where the following symmetry constraint is further imposed on H: $\prod_i X_{a,i} = \prod_i X_{b,i} = 1$ [80].

Now we present the derivation of operator mapping:

$$\begin{aligned}&U Z_{b,i} Z_{b,i+1} U^\dagger \\ &= \sum_{\alpha',\beta',\alpha,\beta}{}^{'} |\alpha',\beta'\rangle\langle\alpha,\beta| \\ &\quad \langle\alpha',\beta'|\, (-1)^{\chi(\alpha',\beta')} Z_{b,i} Z_{b,i+1} (-1)^{\chi(\alpha,\beta)}\, |\alpha,\beta\rangle\,.\end{aligned} \tag{B6}$$

While $Z_{b,i} Z_{b,i+1}$ has no effect on $|\alpha\rangle$ (i.e., $\alpha' = \alpha$), this operator makes the transition from β to β', where β and β' only differ in the site (b,i) and site $(b,i+1)$.

It is not hard to find that the product of the braiding phase $(-1)^{\chi(\alpha',\beta')}(-1)^{\chi(\alpha,\beta)}$, i.e., the braiding sign change induced by $Z_{b,i}Z_{b,i+1}$ is simply equal to α_{i+1}. In other words, $\langle\alpha',\beta'|\,(-1)^{\chi(\alpha',\beta')}Z_{b,i}Z_{b,i+1}(-1)^{\chi(\alpha,\beta)}\,|\alpha,\beta\rangle$

$$\begin{aligned}&= \langle\alpha',\beta'|\,Z_{b,i}\alpha_{i+1}Z_{b,i+1}\,|\alpha,\beta\rangle\\&= \langle\alpha',\beta'|\,Z_{b,i}X_{a,i+1}Z_{b,i+1}\,|\alpha,\beta\rangle\,.\end{aligned}\tag{B7}$$

Therefore, one finds $Z_{b,i}Z_{b,i+1}\rightarrow Z_{b,i}X_{a,i+1}Z_{b,i+1}$. With a similar calculation, one finds $Z_{a,i}Z_{a,i+1}\rightarrow Z_{a,i}X_{b,i}Z_{a,i+1}$.

2. Numerical data on volume-law entropy

Here we report the data on von Neumann entropy of the mixed state ρ_B from the ground state of H [Eq. (9)]. The entropy is defined as $S(\rho_B)=-\mathrm{tr}_B\big[\rho_B\ln(\rho_B)\big]$. The ED calculation for various system sizes is shown in Fig. 6. Our data suggest that $S(\rho_B)$ scales linearly with L, i.e., volume-law scaling, for any nonzero g. In particular, this means that at the critical point $g=1$, B sublattice is a mixed state with volume-law classical entropy coexisting with critical long-range entanglement.

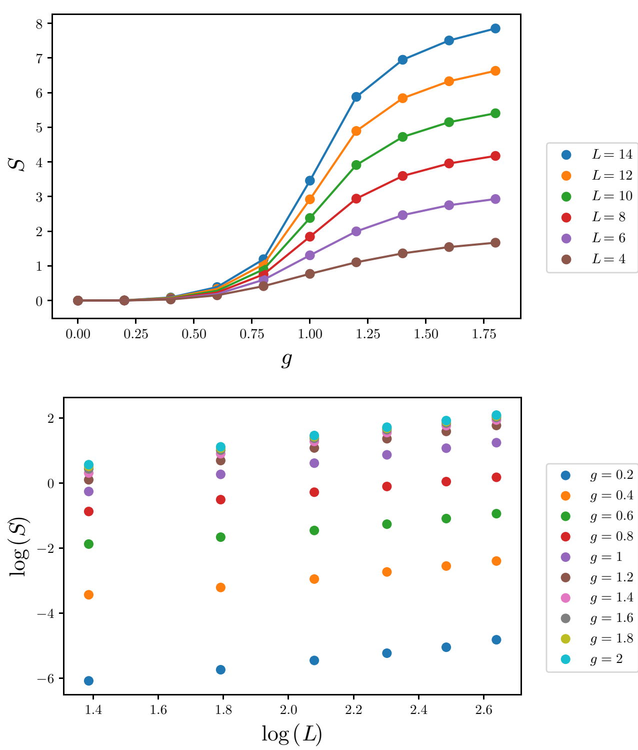

FIG. 6. von Neumann entropy S of the mixed state $\rho_B(=\mathrm{tr}_A\,|\psi\rangle\langle\psi|)$ with $|\psi\rangle$ being the ground state of H in Eq. (9). Upper panel: S as a function of the tuning parameter g. Lower panel: the scaling of S with the system size L of sublattice B. We find S scales linearly with L for any nonzero g.

3. Other nonfixed-point SPT as input

Here we consider various types of symmetric perturbation on the fixed-point $\mathbb{Z}_2\times\mathbb{Z}_2$ SPT, and discuss the structure of the corresponding output state.

On-site X perturbation: here the input is the ground state of the following Hamiltonian:

$$\begin{aligned}H_0 = &-\sum_i Z_{a,i}X_{b,i}Z_{a,i+1}-\sum_i Z_{b,i}X_{a,i+1}Z_{b,i+1}\\&-g\sum_i(X_{a,i}+X_{b,i}).\end{aligned}\tag{B8}$$

The ground state of H_0 belongs to $\mathbb{Z}_2\times\mathbb{Z}_2$ SPT for $g<1$, and belongs to a trivial phase for $g>1$ [81, 82]. Using the transformation rule in Eq. (6), one obtains a Hamiltonian of two decoupled transverse-field Ising chain: $H=H_A+H_B$, where $H_A=-\sum_i Z_{a,i}Z_{a,i+1}-g\sum_i X_{a,i}$ and $H_B=-\sum_i Z_{b,i}Z_{b,i+1}-g\sum_i X_{b,i}$. The state ρ_B from the measurement-feedback channel is the reduced density matrix of the ground state of H by tracing out A. Since A and B are decoupled, ρ_B is in fact a pure state, namely, the ground state of the transverse-field Ising chain, whose long-range order exists for $|g|<1$ (i.e., the regime where the input state is an SPT). In particular, ρ_B being pure means that all postmeasurement state trajectories are transformed to the same state on B with the unitary feedback.

Two-body ZZ perturbation: here the input is the ground state of the Hamiltonian with independently tunable two-body ZZ perturbation on A and B sublattices:

$$\begin{aligned}H_0 = &-\sum_i Z_{a,i}X_{b,i}Z_{a,i+1}-\sum_i Z_{b,i}X_{a,i+1}Z_{b,i+1}\\&-g_A\sum_i Z_{a,i}Z_{a,i+1}-g_B\sum_i Z_{b,i}Z_{b,i+1}.\end{aligned}\tag{B9}$$

The measurement-feedback channel will prepare a state ρ_B on B sublattice with the parent Hamiltonian:

$$\begin{aligned}H = &-\sum_i Z_{a,i}Z_{a,i+1}-\sum_i Z_{b,i}Z_{b,i+1}\\&-g_A\sum_i Z_{a,i}X_{b,i}Z_{a,i+1}-g_B\sum_i Z_{b,i}X_{a,i+1}Z_{b,i+1}.\end{aligned}\tag{B10}$$

H_0 and H are dual to each other, and their phase diagrams are presented in Fig. 7. Interestingly, one notices that with the measurement-feedback channel acting on a gapless state, we can prepare a noncritical mixed state with long-range order. To see this, we consider $g_B=1$ and $g_A<1$. In this case, H_0 exhibits the gapless SPT order [83] since the $\mathbb{Z}_2$ charges on A are used to decorate the domain walls in B sublattice that is tuned to a critical point between a trivial

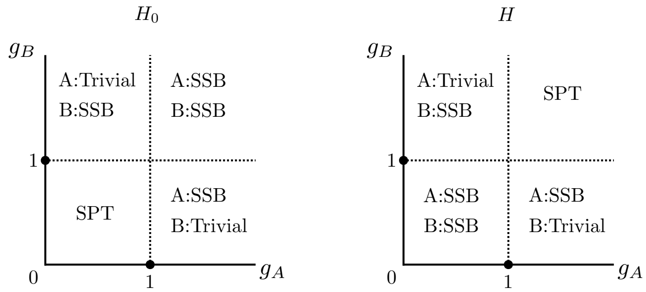

FIG. 7. Phase diagram of H_0 and H defined in Eqs. (B9) and (B10). Taking the ground state of H_0 as an input, the measurement-feedback channel prepares a mixed state on B sublattice, which is the reduced density matrix of the ground state of H.

phase and a $\mathbb{Z}_2$ SSB phase. It follows that by measuring the gapped degrees of freedom on A followed by unitary feedback, one obtains mixed state ρ_B on B sublattice that exhibits a $\mathbb{Z}_2$ SSB order.

More generally, one may consider an input state of the form $|\psi_0\rangle = U |\psi_A\rangle_A |\psi_B\rangle_B$ with $U = \prod CZ_{(a,i),(b,i)} CZ_{(b,i),(a,i+1)}$ being a product of controlled-Z that entangles A and B sublattices. The measurement-feedback protocol will always lead to a mixed state on B with long-range order, as long as $|\psi_0\rangle$ satisfies the following two conditions (in particular $|\psi_0\rangle$ does not need to be an SPT): (1) $|\psi_A\rangle$ is trivial, where domain walls condense (i.e., the product of X along an open string takes a nonzero expectation value c). (2) The input state on B sublattice, i.e., $|\psi_B\rangle$, is invariant under the global $\mathbb{Z}_2$ symmetry: $\prod_{i\in B} X_i |\psi_B\rangle_B = |\psi_B\rangle_B$ (e.g., $|\psi_B\rangle$ can be trivial, spontaneously breaking the symmetry, or critical). The first condition implies that a long-range string operator $\langle\psi_0| Z_B X_A X_A \cdots X_A Z_B |\psi_0\rangle = c$; measuring X_A on A sublattice followed by a unitary feedback acting on B leads to a mixed state ρ_B on B with a long-range ZZ two-point function. (2) The second condition implies that $\mathrm{tr}[\rho \prod_{i\in B} X_i] = 1$. As a result, combining these two conditions already guaranteed the existence of long-range order in the mixed state ρ_B. Practically speaking, it is of best interest of our protocol to consider $|\psi_B\rangle_B$ as a trivial state (in which case $|\psi_0\rangle$ is an SPT), since it furnishes an example of obtaining long-range order only after implementing the protocol.

4. SPT under decoherence as input

In the main text, we discussed a measurement-feedback channel that transforms the string order of the input pure SPT to a long-range order. Specifically, the main result is

$$\mathrm{tr}[\rho Z_{b,i} Z_{b,j}] = \mathrm{tr}[\rho_0 Z_{b,i} \left(\prod_{k=i+1}^{j} X_{a,k}\right) Z_{b,j}], \tag{B11}$$

where $\rho_0 = |\psi_0\rangle\langle\psi_0|$ is the input state. In fact, with a straightforward derivation, one finds the equation holds true for arbitrary input density matrix ρ_0. Namely, ρ_0 needs not be a pure state. As an application, the input state ρ_0 may be a mixed state obtained by subjecting an SPT to certain decoherence channels. If the string order is robust under the channel, the output state of our protocol will remain long-range ordered. Below we will first discuss the decohered SPTs and the corresponding emergent long-range order. We will then discuss the fate of those decohered SPTs when tuned to criticality.

First, we consider a dephasing channel in Pauli-X basis. A local channel is given by $\mathcal{E}_i : \rho \to (1-p)\rho + pX_i\rho X_i = \sum_{\sigma=0,1} p_\sigma K_\sigma^\dagger \rho K_\sigma$ with $K_\sigma = X_i^{\sigma_i}$, and $p_\sigma = p, 1-p$ for $\sigma = 1, 0$ respectively. This can be understood as applying X_i operator with probability p, so $p = 1/2$ corresponds to maximal dephasing. We consider the local channels on every lattice site, so the overall dephasing channel $\mathcal{E}$ is the composition of the local noise channels: $\mathcal{E} = \mathcal{E}_1 \circ \mathcal{E}_2 \circ \cdots \circ \mathcal{E}_{2L}$, and

$$\mathcal{E}[\rho] = \sum_{\boldsymbol{\sigma}} P(\boldsymbol{\sigma}) K_{\boldsymbol{\sigma}}^\dagger \rho K_{\boldsymbol{\sigma}}, \tag{B12}$$

where $\boldsymbol{\sigma} = \{\sigma_i\}$, $P(\boldsymbol{\sigma}) = \prod_{i=1}^{2L} p_{\sigma_i}$, and $K_{\boldsymbol{\sigma}} = \prod_{i=1}^{2L} X_i^{\sigma_i}$. Given a pure SPT, $\rho_{\mathrm{SPT}} = |\phi\rangle\langle\phi|$, the dephasing channel leads to $\rho_0 = \mathcal{E}[\rho_{\mathrm{SPT}}]$, and an operator O with respect to ρ_0 becomes

$$\langle O\rangle_{\rho_0} = \sum_{\boldsymbol{\sigma}} P(\boldsymbol{\sigma}) \langle\phi| K_{\boldsymbol{\sigma}} O K_{\boldsymbol{\sigma}}^\dagger |\phi\rangle . \tag{B13}$$

One immediate consequence is that if $[O, K_{\boldsymbol{\sigma}}] = 0$, then $\langle O\rangle_{\rho_0} = \langle\phi| O |\phi\rangle$, i.e., the expectation value of O remains invariant under the dephasing channel. Therefore, $\left\langle \prod_{i=1}^{L} X_{b,i} \right\rangle_{\rho_0} = 1$ as in $|\phi\rangle$. On the other hand, for the string operator $\mathcal{S} \equiv Z_{b,i} \left(\prod_{k=i+1}^{j} X_{a,k}\right) Z_{b,j}$, since only $Z_{b,i}$ and $Z_{b,j}$ may anticommute with the noise operator $K_{\boldsymbol{\sigma}}$, $\langle\mathcal{S}\rangle_{\rho_0}$ can be simplified as

$$\sum_{\sigma_{b,i}\sigma_{b,j}} p_{\sigma_{b,i}} p_{\sigma_{b,j}} \langle\phi| X_{b,i}^{\sigma_{b,i}} X_{b,j}^{\sigma_{b,j}} \mathcal{S} X_{b,i}^{\sigma_{b,i}} X_{b,j}^{\sigma_{b,j}} |\phi\rangle . \tag{B14}$$

Since the string operator $\mathcal{S}$ conjugated by $X_{b,i}^{\sigma_{b,i}} X_{b,j}^{\sigma_{b,j}}$ acquires a $+1$, -1 sign when $\sigma_{b,i} = \sigma_{b,j}$, $\sigma_{b,i} \neq \sigma_{b,j}$, respectively, one finds

$$\begin{aligned}\langle\mathcal{S}\rangle_{\rho_0} &= \left[\mathrm{Prob.}(\sigma_{b,i} = \sigma_{b,j}) - \mathrm{Prob.}(\sigma_{b,i} \neq \sigma_{b,j})\right] \\ &\quad \times \langle\phi| \mathcal{S} |\phi\rangle \\ &= (1-2p)^2 \langle\phi| \mathcal{S} |\phi\rangle . \end{aligned} \tag{B15}$$

Therefore, under the X-dephasing channel, the string order survives for any nonmaximal dephasing (i.e., $p < 1/2$).

Given this dephased SPT mixed state, one can then use the measurement-feedback channel to obtain a mixed state with GHZ-like long-range order.

If one instead considers the symmetry-breaking dephasing channel based on Pauli-Z noise, with a similar calculation, one finds the resulting dephased state cannot have both $Z_B X_A \cdots X_A Z_B \sim O(1)$ and $\prod_i X_{b,i} = 1$. Specifically, due to the Pauli-Z noise on A sublattice, one finds $Z_B X_A \cdots X_A Z_B \sim (1-2p)^{|S|}$, i.e., exponentially decaying with the length of the string $|S|$ for any nonzero dephasing. On the other hand, the Pauli-Z noise on B sublattice results in $\prod_i X_{b,i} = (1-2p)^L$, i.e., exponentially decaying with sublattice size of B for any nonzero dephasing. As a result, the measurement-feedback channel cannot lead to a mixed state with the GHZ-like long-range order based on such dephased state.

At criticality: when $|\phi\rangle$ is tuned to a critical point [e.g., $g=1$ in Eq. (7)], the string operator exhibits critical order $Z_{b,i}(\prod_{k=i+1}^{j} X_{a,k}) Z_{b,j} \sim 1/|i-j|^{\eta}$. Under the Pauli-$X$ dephasing, with a similar analysis as above, one obtains a mixed state ρ_0 with $\left\langle Z_{b,i}(\prod_{k=i+1}^{j} X_{a,k}) Z_{b,j} \right\rangle_{\rho_0} = (1-2p)^2 \left\langle Z_{b,i}(\prod_{k=i+1}^{j} X_{a,k}) Z_{b,j} \right\rangle_{\text{SPT}} \sim 1/|i-j|^{\eta}$. Therefore, the measurement-feedback channel discussed in Sec. IV A gives rise to a mixed state ρ_B with the critical correlation $Z_{b,i} Z_{b,j} \sim 1/|i-j|^{\eta}$. On the other hand, the disorder operator $X_{b,i} X_{b,i+1} \cdots X_{b,j}$ commutes with both the dephasing channel and the measurement-feedback channel, and therefore, $\langle X_{b,i} X_{b,i+1} \cdots X_{b,j} \rangle_{\rho_0} = \langle X_{b,i} X_{b,i+1} \cdots X_{b,j} \rangle_{\text{SPT}} \sim 1/|i-j|^{2\eta}$. The algebraic order in these operators suggests that ρ_B exhibits critical scaling of entanglement. This is verified with our ED calculation, where the bipartite entanglement negativity follows the universal scaling form as in a 1+1D CFT (see Fig. 8 upper panel):

$$E_N(\alpha, \beta) = \alpha \ln\left(\frac{L}{\pi} \sin\left(\frac{\pi x}{L}\right)\right) + \beta. \qquad \text{(B16)}$$

In particular, the prefactor α decreases as increasing the strength of dephasing.

Another natural question is, given an input dephased SPT ρ_0, what are the typical entanglement structures of the postmeasurement (mixed) state trajectories right after measuring A sublattice? To address this question, we numerically compute the entanglement negativity averaged over these trajectories. As indicated by Fig. 8 lower panel, this quantity also exhibits the critical scaling in entanglement, indicating the pattern of critical entanglement in ρ_B may be attributed to the postmeasurement state trajectories that constitute the ensemble. Note that for a given dephasing strength p, the trajectory-average negativity is always smaller than the negativity in ρ_B. This is consistent with the intuition that some of the long-distance entanglement is diminished by classical fluctuations in the ensemble of those trajectories.

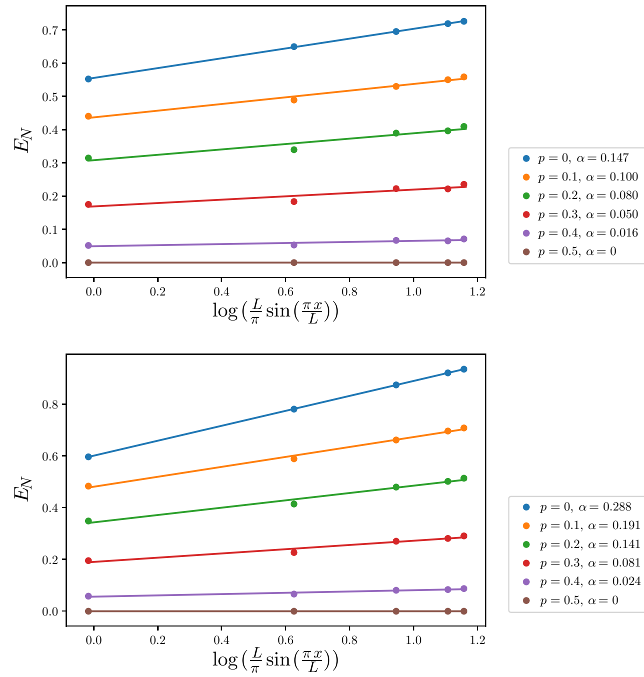

FIG. 8. Entanglement negativity E_N between two complementary segments of size x and $L-x$ on B sublattice for the mixed state ρ_B. The input state is a mixed state ρ_0 obtained by acting the input SPT ψ_0 with a decoherence channel. Upper panel: negativity of ρ_B obtained by the measurement-feedback channel. Lower panel: negativity averaged over mixed-state trajectories obtained by measuring A sublattice for the input dephased SPT ρ_0.

APPENDIX C: MIXED STATE WITH TOPOLOGICAL ORDER FROM MEASURING 2D SPT

Here we discuss a finite-depth protocol that converts higher dimensional SPTs to mixed-state topological orders. In particular, we will consider the input state as a 2D SPT protected by the $\mathbb{Z}_2$ 0-form $\times$ $\mathbb{Z}_2$ 1-form symmetry, in which case the resulting mixed state exhibits a Z_2 topological order.

Consider a 2D lattice with every vertex v and every edge e accommodating a qubit, the fixed-point SPT Hamiltonian reads

$$H_0 = -\sum_v X_v \prod_{e \ni v} Z_e - \sum_e X_e \prod_{v \in e} Z_v. \qquad \text{(C1)}$$

The first term is a product of a Pauli X on vertex v and four neighboring Pauli Zs on edges, and the second term is a product of a Pauli X on edge e and two neighboring Pauli Zs on vertices. This Hamiltonian can be obtained from a trivial paramagnet $-\sum_v X_v - \sum_e X_e$ by a depth-1 unitary circuit $U_{\text{CZ}} = \prod_{\langle v,e \rangle} CZ_{v,e}$, i.e., a product of controlled-Z gates, each of which acts on a pair of neighboring vertex and edge. The ground state is the 2D cluster state, a nontrivial SPT protected by $\mathbb{Z}_2$ 0-form $\times$ $\mathbb{Z}_2$ 1-form symmetry, where the $\mathbb{Z}_2$ 0-form symmetry is given by $\prod_v X_v$ on vertices and the $\mathbb{Z}_2$ 1-form symmetry is given by $\prod_{e\in\gamma} X_e$ acting on edges along any closed loop γ (including noncontractible ones).

The nontrivial SPT order can be diagnosed by the membrane operator $M_{\tilde{\gamma}} = \prod_{e\in\tilde{\gamma}} Z_e \prod_{v\in A_{\tilde{\gamma}}} X_v$, where $\tilde{\gamma}$ is a loop in the dual lattice, and $v \in A_{\tilde{\gamma}}$ denotes all vertices (in the primary lattice) in the area enclosed by the loop $\tilde{\gamma}$. For instance,

$M_{\tilde{\gamma}} =$ 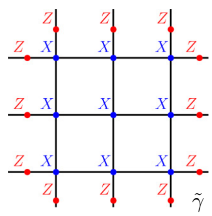

(C2)

For the fixed-point SPT, $\langle M_{\tilde{\gamma}}\rangle = 1$ for any loops $\tilde{\gamma}$. Away from the fixed-point limit, $M_{\tilde{\gamma}}$ exhibits a long-range correlation in the form of a perimeter law: $\langle M_{\tilde{\gamma}}\rangle \sim e^{-c|\tilde{\gamma}|}$. This follows from the decorated domain-wall description of this type of SPT; starting with a trivial paramagnet of Ising spins on vertices, the $\mathbb{Z}_2$ domain walls condense, implying the perimeter law of a domain-wall creation operator $\prod_{v\in A_{\tilde{\gamma}}} X_v \sim e^{-c|\tilde{\gamma}|}$, where $\tilde{\gamma}$ is a closed loop in the dual lattice [84]. We then introduce $\mathbb{Z}_2$ charge on edges to decorate the domain walls by applying U_{CZ}. This leads to an SPT with $M_{\tilde{\gamma}} = \prod_{e\in\tilde{\gamma}} Z_e \prod_{v\in A_{\tilde{\gamma}}} X_v \sim e^{-c|\tilde{\gamma}|}$ because $M_{\tilde{\gamma}}$ is obtained by conjugating the domain-wall operator $\prod_{v\in A_{\tilde{\gamma}}} X_v$ with U_{CZ}.

Now we can utilize the presence of long-range membrane order to devise a protocol for preparing a mixed state with $\mathbb{Z}_2$ topological order. Given an SPT $|\psi_0\rangle$, one measures X_v on all vertices with outcome $\alpha = \{\alpha_v\}$. For each postmeasurement state trajectory with outcome α, one applies a corresponding local unitary U_α acting on edges. This two-step protocol leads to the ensemble $\rho = \sum_\alpha U_\alpha P_\alpha \rho_0 P_\alpha U_\alpha^\dagger$. Using a unitary U_α such that $U_\alpha^\dagger \prod_{e\in\tilde{\gamma}} Z_e U_\alpha = \prod_{e\in\tilde{\gamma}} Z_e \left(\prod_{v\in A_{\tilde{\gamma}}} \alpha_v\right)$, (i.e., the dual loop operator acquires a sign that depends on the measurement outcome enclosed by the loop), the expectation value of loop operators $\prod_{e\in\tilde{\gamma}} Z_e$ in ρ will exactly equal the expectation value of the membrane operator $M_{\tilde{\gamma}} = \prod_{e\in\tilde{\gamma}} Z_e \prod_{v\in A_{\tilde{\gamma}}} X_v$ with respect to the initial input SPT, which exhibits a perimeter-law scaling. In addition, since the symmetry sector is fixed with $\prod_{e\in\gamma} X_e = 1$, the perimeter law scaling indicates a $\mathbb{Z}_2$ topological order on edges in the output mixed state, as in the deconfined phase of a 2+1D $\mathbb{Z}_2$ gauge theory.

Here we discuss the choice of U_α. Due to the global $\mathbb{Z}_2$ symmetry on vertices in the input SPT $|\psi_0\rangle$, the measurement outcomes on vertices satisfy $\prod_v \alpha_v = 1$, i.e., the -1 outcomes will occur in pairs. It turns out U_α is consisting of string operators of Pauli Xs on edges; each string is deformable and connects two $\alpha_v = -1$ outcomes on vertices. Physically, the $\alpha_v = -1$ outcomes may be regarded as e particles in the $\mathbb{Z}_2$ topological order, and U_α is the string operator that annihilates those anyon excitations.

Nontrivialness of the mixed state: now we show that the 1-form symmetry $\prod_{e\in\gamma} X_e = 1$ together with the perimeter law of the Wilson loop in the dual lattice $\prod_{e\in\tilde{\gamma}} Z_e \sim e^{-c|\tilde{\gamma}|}$ implies that the mixed state on edges (ρ_B) is nontrivial; it cannot be a mixture of short-range entangled pure states. This can be proved by contradiction, as discussed in Sec. III. We first assume $\rho_B = \sum_n p_n |n\rangle\langle n|$, where each $|n\rangle$ is a trivial short-range entangled state that can be connected to a product state using a finite-depth local unitary. We define two Wilson loop operators $W_Z(\tilde{\gamma}_i) = \prod_{e\in\tilde{\gamma}_i} Z_e$ for $i = 1, 2$, where $\tilde{\gamma}_1, \tilde{\gamma}_2$ are noncontractible loops around the vertical direction, and they are horizontally separated by a scale $O(d)$, see Fig. 9. For each $|n\rangle$, the connected correlator is $\langle n| W_Z(\tilde{\gamma}_1)W_Z(\tilde{\gamma}_2)|n\rangle_c = \langle n| W_Z(\tilde{\gamma}_1)W_Z(\tilde{\gamma}_2)|n\rangle - \langle n| W_Z(\tilde{\gamma}_1)|n\rangle \langle n| W_Z(\tilde{\gamma}_1)|n\rangle$. Due to the 1-form symmetry $W_X(\gamma) = \prod_{e\in\gamma} X_e = 1$ with γ winding around torus horizontally, $\langle n| W_Z(\tilde{\gamma}_i)|n\rangle = 0$ for both $i = 1, 2$. On the other hand, the connected correlator in the trivial state $|n\rangle$ decays exponentially with d [85], and correspondingly $\langle n| W_Z(\tilde{\gamma}_1)W_Z(\tilde{\gamma}_2)|n\rangle$ decays with the separation d as well. This in turn implies the $W_Z(\tilde{\gamma}_1)W_Z(\tilde{\gamma}_2)$ decays with d in the ensemble of $|n\rangle$, which contradicts the perimeter law scaling $W_Z(\tilde{\gamma}_1)W_Z(\tilde{\gamma}_2) \sim e^{-\alpha L}$, which does not decay with

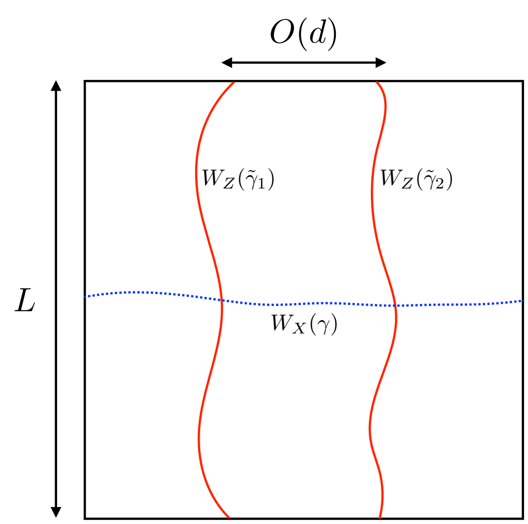

FIG. 9. On a 2D lattice of size $L \times L$ on the surface of a 2-torus (by imposing periodic boundary conditions), the perimeter law decay of the Wilson loops in the dual lattice and the 1-form symmetry in the primary lattice together imply a nontrivial mixed state.

d in the output mixed state. Therefore, the assumption that ρ_B is a mixture of trivial states must be false.

Structure of mixed state topological order: here we discuss the structure of the topologically ordered mixed state using a wave-function perspective. This allows us to derive a duality transformation that facilitates the characterization of the phase diagram of the mixed state as varying the input state.

First, we express the input state in Pauli-X basis:

$$|\psi_0\rangle = \sum_{\alpha,\beta}{}' (-1)^{\chi(\alpha,\beta)} \psi(\alpha,\beta)\,|\alpha,\beta\rangle \tag{C3}$$

$\alpha = \{\alpha_v\}$ and $\beta = \{\beta_e\}$ denote the configurations in X basis for qubits on vertices and edges, respectively. $\sum'_{\alpha,\beta}$ denotes summing all symmetry-allowed α, β configurations: the global symmetry on vertices implies $\alpha_v = -1$ occurs in pairs, so every allowed α configuration corresponds to the configuration of open strings whose end points label the location of $\alpha_v = -1$. On the other hand, the 1-form symmetry on edges indicates the edge with $\beta_e = -1$ must form a closed loop in the dual lattice, which equivalently can be regarded as the boundary of an open membrane. $\chi(\alpha,\beta)$ is the number of times that the α strings pierce through the β membranes. When $|\psi_0\rangle$ is a fixed-point SPT, $\psi(\alpha,\beta)$ is independent of α, β (see Fig. 10).

With the input state $|\psi_0\rangle$, measuring vertices (A sublattice) projects to a particular α configuration, and the follow-up unitary correction U_α removes the braiding phase. One then finds the measurement-feedback protocol leads to a mixed state ρ_B on the edges (B sublattice), which is the reduced density matrix (by tracing out A sublattice) of the following state:

$$|\psi\rangle = \sum_{\alpha,\beta}{}' \psi(\alpha,\beta)\,|\alpha,\beta\rangle\,. \tag{C4}$$

Therefore, the input state and the purification of the output ρ_B can be connected through $|\psi\rangle = U|\psi_0\rangle$, where $U = \sum'_{\alpha,\beta} |\alpha,\beta\rangle\langle\alpha,\beta|\,(-1)^{\chi(\alpha,\beta)}$ is unitary in the symmetric subspace. Under the conjugation of U, operators transform as

$$\begin{gathered} X_v \to X_v, \quad X_e \to X_e, \\ \prod_{e\ni v} Z_e \to X_v \prod_{e\ni v} Z_e, \quad \prod_{v\in e} Z_v \to X_e \prod_{v\in e} Z_v. \end{gathered} \tag{C5}$$

This allows us to derive the parent Hamiltonian H of $|\psi\rangle$ from the Hamiltonian H_0 of the input state via $H = UH_0U^\dagger$. Also, note that $|\psi\rangle$ lives in the subspace given by 0-form symmetry $\prod_v X_v = 1$ and $\mathbb{Z}_2$ 1-form symmetry $\prod_{e\in\gamma} X_e = 1$ (acting on edges along any closed loop γ), these two constraints need to be further imposed in H.

As an application, we may consider perturbing the fixed-point SPT by onsite Pauli Xs: $H_0 = -\sum_v X_v \prod_{e\ni v} Z_e - \sum_e X_e \prod_{v\in e} Z_v - g\sum_e X_e - g\sum_v X_v$, the corresponding H is the decoupled Ising model on vertices and 2D toric code, both of which are subject to the onsite transverse field: $H = -\sum_v \prod_{e\ni v} Z_e - \sum_e \prod_{v\in e} Z_v - g\sum_e X_e - g\sum_v X_v$, where the constraints $\prod_v X_v = 1$ and $\prod_{e\in\gamma} X_e = 1$ are further imposed. Therefore, the measurement-feedback protocol leads to a pure state ρ_B on edges with $\mathbb{Z}_2$ topological order. This also indicates all possible postmeasurement states by measuring the input state SPT $|\psi_0\rangle$ are deterministically converted to the same pure state with topological order.

To discuss a nontrivial mixed-state topological order on edges, we consider the following form of input Hamiltonian:

$$\begin{aligned} H_0 = &-\sum_v X_v \prod_{e\ni v} Z_e - \sum_e X_e \prod_{v\in e} Z_v \\ &- g\sum_v \prod_{e\ni v} Z_e - g\sum_e \prod_{v\in e} Z_v. \end{aligned} \tag{C6}$$

Using the transformation rule in Eq. (C5), one finds the corresponding H

$$\begin{aligned} H = &-\sum_v \prod_{e\ni v} Z_e - \sum_e \prod_{v\in e} Z_v \\ &- g\sum_v X_v \prod_{e\ni v} Z_e - g\sum_e X_e \prod_{v\in e} Z_v, \end{aligned} \tag{C7}$$

where the 0-form symmetry ($\prod_v X_v = 1$) and 1-form symmetry ($\prod_{e\in\gamma} X_e = 1$) are further imposed. To understand

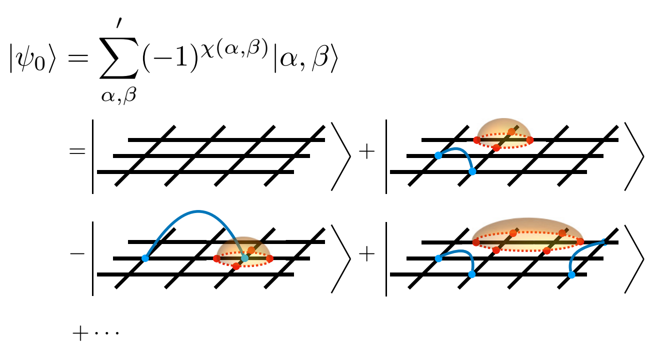

FIG. 10. Wave function of the $\mathbb{Z}_2 \times \mathbb{Z}_2$ fixed-point SPT, i.e., the ground state of $H_0 = -\sum_v X_v \prod_{e\ni v} Z_e - \sum_e X_e \prod_{v\in e} Z_v$. The fixed-point state is understood as a condensate of open blue strings and open red membranes with a nontrivial braiding sign structure in Pauli-X basis. The wave function $(-1)^{\chi(\alpha,\beta)}$ takes the value 1 (-1) corresponding to the even (odd) number of times that blue strings pierce through red membranes.

the phase diagram for the mixed state ρ_B defined on edges, we transform H by $U_{\mathrm{CZ}} = \prod_{\langle v,e\rangle} \mathrm{CZ}_{v,e}$. This leads to

$$-\sum_v \prod_{e\ni v} Z_e - \sum_e \prod_{v\in e} Z_v - g\sum_v X_v - g\sum_e X_e, \quad \text{(C8)}$$

i.e., a transverse-field Ising model on vertices and transverse-field toric code on edges. Their phase diagrams are well understood: the global Ising symmetry breaking order persists to $g = g_{\mathrm{Ising}} \approx 3.04438$ [86], above which the state on vertices become trivial. On the other hand, using the (Kramer-Wannier) duality between transverse-field Ising and transverse-field toric code, the topological order persists up to $g = g_{\mathrm{toric}} = 1/g_{\mathrm{Ising}} \approx 0.32847$, above which the state on edges become trivial. As a result, starting with the ground state $|\psi_0\rangle$ of Eq. (C6) for $g < g_{\mathrm{toric}}$ (the regime where $|\psi_0\rangle$ is an SPT), the measurement-feedback channel gives a mixed state ρ_B on edges with $\mathbb{Z}_2$ topological order. Similar to the discussion in 1D, one expects ρ_B to have volume-law entropy due to the coupling between A, B sublattices in Eq. (C7).

Finally, we note that mixed-state topological order encoded in ρ_B may be diagnosed by entanglement negativity, an entanglement measure for mixed states. In particular, one expects a long-range entanglement structure that manifests in the universal subleading contribution in negativity as discussed in Refs. [4,5,11].

APPENDIX D: FERMIONIC MIXED STATE WITH KITAEV TOPOLOGICAL ORDER IN 1D

Here we discuss the finite-depth preparation of a mixed state in 1D that exhibits a topological order of the Kitave Majorana chain [87,88] by taking a $\mathbb{Z}_2 \times \mathbb{Z}_2^f$ SPT $|\psi_0\rangle$ [20,59–62] as an input. Here we closely follow Ref. [20] to construct the fixed-point SPT, and then we will consider certain symmetric perturbation and apply measurement and unitary feedback to prepare a nontrivial fermionic topological mixed state.

To start, we consider a 1D lattice of size $2L$ initialized in a product state, see Fig. 11(a): every odd site accommodates a qubit initiated in the $|+\rangle$ state, and every even site accommodates a fermion initiated in the empty state, i.e., parity operator $P = -i\gamma\gamma' = 1 - 2c^\dagger c = 1$ with left Majorana and right Majorana defined as $\gamma = c + c^\dagger, \gamma' = -i(c - c^\dagger)$. Define a Majorana hopping operator $S_{2n} = i\gamma'_{2n-2}\gamma_{2n}$, we define a controlled gate

$$CS_{2n-1} = |\uparrow\rangle\langle\uparrow| + |\downarrow\rangle\langle\downarrow| S_{2n}; \quad \text{(D1)}$$

the Majorana hops from the site $2n-2$ to site $2n$ only when the qubit at $2n-1$ is in the spin-down state. Using

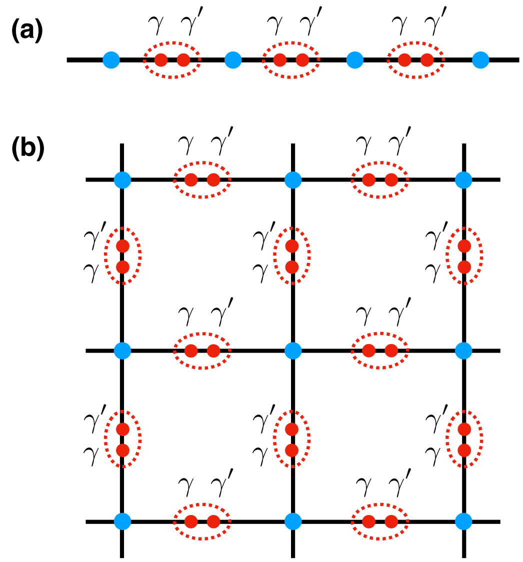

FIG. 11. (a) 1D lattice with every odd site accommodating a qubit and every even site accommodating two Majorana fermions. Given an initial 0-form $\mathbb{Z}_2 \times \mathbb{Z}_2^f$ SPT, measurement and unitary feedback lead to a fermionic mixed state with the topological phase of the Kitaev chain. (b) 2D lattice with every vertex accommodating a qubit and every edge accommodating two Majorana fermions. Given an initial $\mathbb{Z}_2$ 0-form $\times\mathbb{Z}_2^f$ 1-form SPT, measurement and unitary feedback leads to a fermionic mixed state with $\mathbb{Z}_2$ topological order.

CS gate, one introduces a depth-1 local unitary circuit

$$U_{\mathrm{SPT}} = \prod_{n=1}^{L} CS_{2n-1}. \quad \text{(D2)}$$

Applying U_{SPT} on the initial product state will then lead to the $\mathbb{Z}_2 \times \mathbb{Z}_2^f$ fixed-point SPT $|\psi_0\rangle$. Equivalently, $|\psi_0\rangle$ is uniquely specified by the stabilizers

$$\begin{aligned} U_{\mathrm{SPT}} X_{2n-1} U_{\mathrm{SPT}}^\dagger &= i\gamma'_{2n-2} X_{2n-1}\gamma_{2n} \\ U_{\mathrm{SPT}} P_{2n} U_{\mathrm{SPT}}^\dagger &= Z_{2n-1} P_{2n} Z_{2n+1}. \end{aligned} \quad \text{(D3)}$$

The SPT $|\psi_0\rangle$ is protected by the $\mathbb{Z}_2 \times \mathbb{Z}_2^f$ symmetry, where $\mathbb{Z}_2$ action is given by the product of X_n on odd sites, and $\mathbb{Z}_2^f$ action is given by the product of P_n on even sites. The state has long-range string order diagnosed by $i\gamma'_{2n-2}X_{2n-1}\gamma_{2n} i\gamma'_{2n}X_{2n+1}\gamma_{2n+2}\cdots i\gamma'_{2m-2}X_{2m-1}\gamma_{2m} = 1$ (this is simply the product of stabilizers). Being a nontrivial SPT, the string order is robust under weak symmetric perturbations, and it approaches a finite constant c with $0 < c < 1$ in the limit $|m-n| \to \infty$.

Given a nonfixed point SPT, as in the discussion for 1D $\mathbb{Z}_2 \times \mathbb{Z}_2$ bosonic SPT, we measure Pauli Xs on all spins on odd sites and record the outcome $\alpha = \{\alpha_i | \text{odd } i\}$. For each postmeasurement state, one applies unitary feedback, i.e., a product of on-site fermionic parity operators:

$$U_\alpha = \prod_{n=1}^{L} P_{2n}^{\frac{1-\prod_{m=1,2,\ldots}^{n} \alpha_{2m-1}}{2}}, \tag{D4}$$

namely, a parity operator at site $2n$ is applied when there is an odd number of -1 outcomes among $\alpha_1, \alpha_3, \ldots, \alpha_{2n-1}$. With this, one obtains a mixed state of Majorana fermions with the long-range order $i\gamma'_{2n-2}\gamma_{2n} i\gamma'_{2n}\gamma_{2n+2} \cdots i\gamma'_{2m-2}\gamma_{2m} = c$, which is a universal feature in the topological phase of a 1D Kitaev chain [87].

Wave-function perspective. It is useful to discuss the above result from the wave-function perspective. As in the $\mathbb{Z}_2 \times \mathbb{Z}_2$ fixed-point bosonic SPT, the $\mathbb{Z}_2 \times \mathbb{Z}_2^f$ fixed-point SPT can also be understood as the condensate of strings with a braiding structure. Specifically, the fixed point $|\psi_0\rangle$ can be written as

$$|\psi_0\rangle = \sum_{\alpha,\beta}{}' (-1)^{\chi(\alpha,\beta)} |\alpha, \beta\rangle, \tag{D5}$$

where $\alpha = \{\alpha_i \in \{\pm 1\}\}$ denotes the product state in Pauli-X basis for qubits and $\beta = \{\beta_i \in \{\pm 1\}\}$ denotes the product state basis with definite fermion parity on even sites [89]. The $\mathbb{Z}_2$ symmetry and $\mathbb{Z}_2^f$ symmetry implies $\prod_{\text{odd } i} \alpha_i = 1$ and $\prod_{\text{even } i} \beta_i = 1$, respectively. As α_i comes in pairs, an α configuration may be represented by open strings (A strings) whose boundary points label $\alpha_i = -1$. Similarly one can define B strings to represent product state basis β for fermions. $\chi(\alpha, \beta)$ is the number of times that A strings and B strings intersect.

Away from the fixed point, one can write $|\psi_0\rangle = \sum'_{\alpha,\beta} (-1)^{\chi(\alpha,\beta)} \psi(\alpha, \beta) |\alpha, \beta\rangle$ and the corresponding measurement-feedback channel gives the mixed states of fermion ρ_B, which is the reduced density matrix of $|\psi\rangle = \sum'_{\alpha,\beta} \psi(\alpha, \beta) |\alpha, \beta\rangle$ by tracing out qubits on odd sites.

$|\psi\rangle$ and $|\psi_0\rangle$ can be connected by the unitary $U = \sum'_{\alpha,\beta} |\alpha, \beta\rangle \langle \alpha, \beta| (-1)^{\chi(\alpha,\beta)}$ [90], which has the action that

$$\begin{aligned} X_{2n-1} &\to X_{2n-1}, \quad P_{2n} \to P_{2n}, \\ Z_{2n-1}Z_{2n+1} &\to Z_{2n-1}P_{2n}Z_{2n+1}, \\ \gamma'_{2n-2}\gamma_{2n} &\to \gamma'_{2n-2}X_{2n-1}\gamma_{2n}. \end{aligned} \tag{D6}$$

As an application, we consider the initial Hamiltonian $H_0 = -\sum_n (i\gamma'_{2n-2}X_{2n-1}\gamma_{2n} + Z_{2n-1}P_{2n}Z_{2n+1}) - g \sum_n (i\gamma'_{2n-2}\gamma_{2n} + Z_{2n-1}Z_{2n+1})$. To understand the phase diagram, we may use the depth-1 unitary circuit [Eq. (D2)] and find $UH_0U^\dagger = -\sum_n (X_{2n-1} + P_{2n}) - g \sum_n (i\gamma'_{2n-2}\gamma_{2n} + Z_{2n-1}Z_{2n+1})$, which is a transverse-field Ising chain on odd sites, and fermionic Kitaev chain on even sites. Consequently, for $|g| < 1$, both sublattices are trivial, while for $|g| > 1$, odd sites exhibit a $\mathbb{Z}_2$ symmetry-breaking order and even sites belong to the topological phase of Kitaev chain. This implies the ground state of H_0 exhibits the $\mathbb{Z}_2 \times \mathbb{Z}_2^f$ SPT order for $|g| < 1$, and for $|g| > 1$, odd sites exhibit $\mathbb{Z}_2$ symmetry-breaking order and even sites belong to the fermionic topological phase.

With the measurement-feedback channel, one obtains a state ρ_B of fermions, which is the reduced density matrix of the ground state $|\psi\rangle$ of H:

$$\begin{aligned} H = &-\sum_n (i\gamma'_{2n-2}\gamma_{2n} + Z_{2n-1}Z_{2n+1}) \\ &- g \sum_n (i\gamma'_{2n-2}X_{2n-1}\gamma_{2n} + Z_{2n-1}P_{2n}Z_{2n+1}). \end{aligned} \tag{D7}$$

H is exactly dual to H_0. As a result, the measurement-feedback channel acting on the pure state of the SPT phase (Kitaev topological phase) leads to the Kitaev topological phase (trivial phase) in the mixed state defined on even sites. Note that for $|\psi_0\rangle$ belonging to the Kitaev topological phase, $|\psi\rangle$ is a nontrivial SPT, but tracing out odd sites leads to a trivial reduced density matrix on even sites.

APPENDIX E: FERMIONIC MIXED STATE WITH TOPOLOGICAL ORDER IN 2D

One may generalize the discussion above to higher space dimensions, which allows for the existence of (non-invertible) topological order in fermionic systems [91].

Consider a 2D lattice with every vertex accommodating a qubit and every edge accommodating two Majorana fermions [see Fig. 11(b)], we can construct a fixed-point SPT with $\mathbb{Z}_2$ 0-form $\times$ $\mathbb{Z}_2^f$ 1-form symmetry as follows. We introduce Majorana hopping operators $S_{v,\to}$ which take the form $i\gamma'\gamma$, where γ', γ are the Majoranas in the left and right of the vertex v. Similarly, the operators $S_{v,\uparrow}$ take the form $i\gamma'\gamma$, where γ', γ are the Majoranas right above and below the vertex v. Using the Majorana hopping operators, one defines a controlled gate

$$CS_v = |\uparrow\rangle\langle\uparrow| + |\downarrow\rangle\langle\downarrow| S_{v,\to}S_{v,\uparrow}. \tag{E1}$$

Starting with a product state, where qubits are in $|+\rangle$ and fermions are in product states with definite fermion parity $P = 1$, simultaneously applying CS_v on all vertices leads to the SPT $|\psi_0\rangle$, which is uniquely specified by the stabilizers ZP_eZ (the product of a fermion parity on the edge e and two Pauli Z on two vertices on the boundary of e), and $X_{2n-1}\gamma'\gamma'\gamma\gamma$ (i.e., the product of and a Pauli X at the vertex v and four Majoranas around v counterclockwise). The SPT is protected by a $\mathbb{Z}_2^f$ 1-form symmetry ($\prod_{e\in C} P_e$, i.e., the product of fermion parity along any loops) and $\mathbb{Z}_2$ 0-form symmetry ($\prod_v X_v$). In particular, the nontrivialness of the SPT manifests in the membrane operator

$M_{\tilde{C}} = \prod_{e\in\tilde{C}} \tilde{\gamma} \prod_{v\in A_{\tilde{C}}} X_v = 1$, where $\prod_{e\in\tilde{C}} \tilde{\gamma}$ is the product of Majoranas ($\tilde{\gamma}$ could be γ or γ') along a loop in the dual lattice, and $\prod_{v\in A_{\tilde{C}}} X_v$ is the product of X_v in the area enclosed by the loop $\tilde{C}$. For instance,

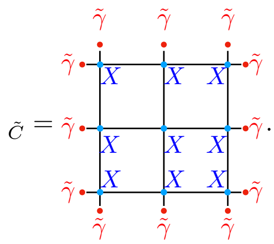

(E2)

For nonfixed-point SPT, the membrane operator will survive in the form of a perimeter law $\langle M_{\tilde{C}} \rangle \sim e^{-\mu|\tilde{C}|}$. With the protocol of first measuring X_v on every vertex, followed by a unitary correction, one obtains an output mixed state ρ with $\mathrm{tr}[\rho \prod_{e\in\tilde{C}} \tilde{\gamma}] \sim e^{-\mu|\tilde{C}|}$. This perimeter law of the loop in the dual lattice together with the 1-form symmetry $\prod_{e\in C} P_e = 1$, which inherits from the input SPT, in the primary lattice indicates a topological order consisting of Majorana fermions. When the input SPT is a fixed-point state, the output reduces to a pure state, which is exactly a ground state of the Majorana surface code discussed in Ref. [92].

APPENDIX F: PURIFICATION OF THE MIXED STATE FROM MEASURING 1D FREE FERMIONS

In Sec. V A we discussed a measurement-feedback protocol that leads to a mixed state ρ with an enhanced spin-spin correlation. Here we discuss the structure of ρ, and in particular, by unveiling a novel braiding structure between "spin" and "charge" in the initial input state $|\psi_0\rangle$, ρ can be purified as a ground state of a local Hamiltonian H, which we derive below.

To begin with, instead of using the conventional occupation-number basis, we will consider the basis that manifests the structure of "spin" and "charge." For simplicity, let us first consider the i'th lattice site as an example. This single site is ssociated to a 4-dim Hilbert space spanned by $|0\rangle, |\uparrow\rangle = c^\dagger_{i,\uparrow}|0\rangle, |\downarrow\rangle = c^\dagger_{i,\downarrow}|0\rangle, |\uparrow\downarrow\rangle = c^\dagger_{i,\uparrow}c^\dagger_{i,\downarrow}|0\rangle$. In the 2-dim subspace with single-fermion occupation number, i.e., spanned by $|\uparrow\rangle, |\downarrow\rangle$, one can define two orthonormal states $(|\uparrow\rangle \pm |\downarrow\rangle)/\sqrt{2}$ as the symmetric and antisymmetric superposition of spin up and spin down, i.e., the eigenstates of the spin-flip operator $\mathcal{S}^x_i = 2S^x_i$. Therefore, denoting the fermion occupation number as $n_i = n_{i,\uparrow} + n_{i,\downarrow}$, one can define the complete basis states $|n_i = 0\rangle$, $|n_i = 2\rangle$, $|n_i = 1, \beta_i = 1\rangle$, $|n_i = 1, \beta_i = -1\rangle$, where $\beta = \pm 1$ corresponds to the eigenvalues of the spin-flip operator $\mathcal{S}^x_i$. As a more compact notation, the basis may be defined as $|n_i, \beta_i\rangle$ with $n_i \in \{0, 1, 2\}$ and $\beta_i \in \{\pm 1\}$, and importantly, β_i degree of freedom exists only when $n_i = 1$. Generalizing the discussion to all lattice sites, one constructs the basis [93] $|n, \beta\rangle$ with $n \equiv \{n_i\}, \beta \equiv \{\beta_i\}$, and the input fermionic pure state may be written as

$$|\psi_0\rangle = \sum_{n,\beta}{}' (-1)^{\chi(n,\beta)} \psi(n,\beta) |n,\beta\rangle . \tag{F1}$$

Since β_i exists only when $n_i = 1$, the β configuration must be consistent with fermion number configuration n. Alternatively, this consistency condition can be imposed on the wave function so that $\psi(n, \beta) = 0$ when β is not consistent with n. In addition to the above consistency condition, for the summation $\sum'_{n,\beta}$, the allowed n, β must respect the global $\mathbb{Z}_2 \times \mathbb{Z}_2$ symmetry as a consequence of the equal number of up-spins and down-spins in $|\psi_0\rangle$. The first $\mathbb{Z}_2$ corresponds the fermion parity symmetry: the total fermion number N must be even since $N = N_\uparrow + N_\downarrow = 2N_\uparrow$. This implies configuration n must satisfy $\prod_i (-1)^{n_i} = 1$, so the number of lattice sites with a single occupation number (odd fermion parity) must be even. The second $\mathbb{Z}_2$ corresponds to the global spin flip given by $\prod_i \mathcal{S}^x_i$, so the product of β_i (at the site with $n_i = 1$) must be one. This means $\beta_i = -1$ comes in pairs. Since both $n_i = 1$ (odd fermion parity) and $\beta_i = -1$ come in pairs, with the ordering $n_1, \beta_1, n_2, \beta_2, \ldots$ along a 1D line, one can use strings to label the configurations of $n_i = 1, \beta_i = -1$, and define a braiding sign structure between charge n and spin β, as in the bosonic $\mathbb{Z}_2 \times \mathbb{Z}_2$ SPT discussed in Appendix B 1.

Given Eq. (F1), measuring global fermion occupation number gives $P_n |\psi_0\rangle = \sum'_\beta (-1)^{\chi(n,\beta)} \psi(n, \beta) |n, \beta\rangle$. As one can check, the unitary feedback $U_n = \prod_{i=1}^{L} \left(\mathcal{S}^x_i\right)^{\sum_{j\le i} n_j}$ [Eq. (15)] removes the braiding sign: $U_n P_n |\psi_0\rangle = \sum'_\beta \psi(n, \beta) |n, \beta\rangle$, and therefore, the resulting mixed state is

$$\begin{aligned} \rho &= \sum_n{}' U_n P_n |\psi_0\rangle \langle\psi_0| P_n U_n^\dagger \\ &= \sum_{\beta,\beta'}{}' \left[\sum_n{}' \psi(n,\beta)\psi(n,\beta') \right] |n,\beta\rangle \langle n,\beta'| . \end{aligned} \tag{F2}$$

Since only the spin sector carries long-range correlation, one may consider the reduced density matrix in the spin sector by tracing out the charge sector, which leads to $\rho_s = \sum'_{\beta,\beta'} \left[\sum'_n \psi(n, \beta)\psi(n, \beta')\right] |\beta\rangle \langle\beta'|$. This is nothing but the reduced density matrix of

$$|\psi\rangle = \sum_{n,\beta}{}' \psi(n,\beta) |n,\beta\rangle . \tag{F3}$$

To better characterize the structure of $|\psi\rangle$, one can derive its parent Hamiltonian. This is achieved by finding the unitary U such that $|\psi\rangle = U|\psi_0\rangle$. Then the parent Hamiltonian H of $|\psi\rangle$ can be obtained by $H = UH_0U^\dagger$, where H_0 is the parent Hamiltonian of the spinful free fermion state $|\psi_0\rangle$, namely, $H_0 = -\sum_{i,\sigma}(c^\dagger_{i+1,\sigma}c_{i,\sigma} + \text{h.c.})$. By comparing $|\psi_0\rangle$ [Eq. (F1)] and $|\psi\rangle$ [Eq. (F3)], U may be chosen as

$$U = \sum_{n,\beta}{}' |n,\beta\rangle\langle n,\beta|(-1)^{\chi(n,\beta)}. \tag{F4}$$

U is diagonal in the basis $|n,\beta\rangle$ with the diagonal entries encoding the braiding phases. While U is not a unitary in the entire Hilbert space, it is a unitary in the restricted Hilbert space with the $\mathbb{Z}_2\times\mathbb{Z}_2$ symmetry. Alternatively, U may be written as $U = \prod_{i=1}^{L}\left(\mathcal{S}^x_i\right)^{\sum_{j\le i}\hat{n}_j}$, which is the same as Eq. (F4) in the symmetric subspace. We note that $\hat{n}_j$ is a number operator instead of a c number. U allows us to derive the parent Hamiltonian of $|\psi\rangle$ through $H = UH_0U^\dagger$:

$$\begin{aligned} H = -\sum_{i,\sigma}\Big[& c^\dagger_{i+1,\sigma}c_{i,\sigma}P_{n_i+n_{i+1}\neq 2} \\ & + c^\dagger_{i+1,\sigma}c_{i,-\sigma}P_{n_i+n_{i+1}=2}P_{n_i=1} \\ & - c^\dagger_{i+1,\sigma}c_{i,-\sigma}P_{n_i+n_{i+1}=2}P_{n_i=2}\Big] + \text{h.c.}, \end{aligned} \tag{F5}$$

where P is a projector with a subscript that labels the subspace it projects to, and the constraint $\prod_i(-1)^{n_i} = \prod_i\mathcal{S}^x_i = 1$ is further imposed on H.

Below we present the derivation of H: consider the term $c^\dagger_{i+1,\uparrow}c_{i,\uparrow}$, it transforms as $Uc^\dagger_{i+1,\uparrow}c_{i,\uparrow}U^\dagger$. To proceed, we compute the matrix entries of this matrix:

$$\begin{aligned} & \langle n',\beta'|Uc^\dagger_{i+1,\uparrow}c_{i,\uparrow}U^\dagger|n,\beta\rangle \\ & = \langle n',\beta'|(-1)^{\chi(n',\beta')}c^\dagger_{i+1,\uparrow}c_{i,\uparrow}(-1)^{\chi(n,\beta)}|n,\beta\rangle. \end{aligned} \tag{F6}$$

Since the fermion hops from ith site to $i+1$th site, there are only four possible cases for obtaining nonvanishing values: $(n_i,n_{i+1}) = (2,1)$, $(n_i,n_{i+1}) = (1,0)$, $(n_i,n_{i+1}) = (2,0)$, $(n_i,n_{i+1}) = (1,1)$. Below we separately discuss these cases.

Case (a) $(n_i,n_{i+1}) = (2,1)$: in this case, one finds the fermion hopping does not change the braiding phase, namely, $(-1)^{\chi(n',\beta')}(-1)^{\chi(n',\beta')} = 1$. Therefore, $\langle n',\beta'|(-1)^{\chi(n',\beta')}c^\dagger_{i+1,\uparrow}c_{i,\uparrow}(-1)^{\chi(n,\beta)}|n,\beta\rangle = \langle n',\beta'|c^\dagger_{i+1,\uparrow}c_{i,\uparrow}|n,\beta\rangle$. Alternatively, one can replace the braiding phase $(-1)^{\chi(n,\beta)}$ with the operator $\prod_{i=1}^{L}\left(\mathcal{S}^x_i\right)^{\sum_{j\le i}\hat{n}_j}$, and go through the algebra to derive the same result.

Case (b) $(n_i,n_{i+1}) = (1,0)$: as in case (a), in this case, one finds the fermion hopping does not change the braiding phase as well. Therefore, $\langle n',\beta'|(-1)^{\chi(n',\beta')}c^\dagger_{i+1,\uparrow}c_{i,\uparrow}(-1)^{\chi(n,\beta)}|n,\beta\rangle = \langle n',\beta'|c^\dagger_{i+1,\uparrow}c_{i,\uparrow}|n,\beta\rangle$.

Case (c) $(n_i,n_{i+1}) = (2,0)$: in this case, after the fermion hopping, both ith site and $i+1$th site contain a single fermion. It follows that the braiding sign will change when $\beta'_i = -1$. Therefore, $\langle n',\beta'|(-1)^{\chi(n',\beta')}c^\dagger_{i+1,\uparrow}c_{i,\uparrow}(-1)^{\chi(n,\beta)}|n,\beta\rangle = \langle n',\beta'|\beta'_ic^\dagger_{i+1,\uparrow}c_{i,\uparrow}|n,\beta\rangle = \langle n',\beta'|\mathcal{S}^x_i c^\dagger_{i+1,\uparrow}c_{i,\uparrow}|n,\beta\rangle$. Writing $\mathcal{S}^x_i = c^\dagger_{i,\uparrow}c_{i,\downarrow} + c^\dagger_{i,\downarrow}c_{i,\uparrow}$, the result can be simplified as $\langle n',\beta'|(-1)^{\chi(n',\beta')}c^\dagger_{i+1,\uparrow}c_{i,\uparrow}(-1)^{\chi(n,\beta)}|n,\beta\rangle = \langle n',\beta'|(-c^\dagger_{i+1,\uparrow}c_{i,\downarrow})|n,\beta\rangle$.

Case (d) $(n_i,n_{i+1}) = (1,1)$: in this case, the braiding sign will change if before hopping, $\beta_i = -1$. Therefore, $\langle n',\beta'|(-1)^{\chi(n',\beta')}c^\dagger_{i+1,\uparrow}c_{i,\uparrow}(-1)^{\chi(n,\beta)}|n,\beta\rangle = \langle n',\beta'|c^\dagger_{i+1,\uparrow}c_{i,\uparrow}\beta_i|n,\beta\rangle = \langle n',\beta'|c^\dagger_{i+1,\uparrow}c_{i,\uparrow}\mathcal{S}^x_i|n,\beta\rangle$. Using the representation $\mathcal{S}^x_i = c^\dagger_{i,\uparrow}c_{i,\downarrow} + c^\dagger_{i,\downarrow}c_{i,\uparrow}$, one finds $\langle n',\beta'|(-1)^{\chi(n',\beta')}c^\dagger_{i+1,\uparrow}c_{i,\uparrow}(-1)^{\chi(n,\beta)}|n,\beta\rangle = \langle n',\beta'|c^\dagger_{i+1,\uparrow}c_{i,\downarrow}|n,\beta\rangle$.

By combining the discussion on these four cases, one obtains the parent Hamiltonian in Eq. (F5).

[1] S. Bravyi and B. Terhal, A no-go theorem for a two-dimensional self-correcting quantum memory based on stabilizer codes, New J. Phys. **11**, 043029 (2009).

[2] M. B. Hastings, Topological Order at Nonzero Temperature, Phys. Rev. Lett. **107**, 210501 (2011).

[3] B. Yoshida, Feasibility of self-correcting quantum memory and thermal stability of topological order, Ann. Phys. (N. Y) **326**, 2566 (2011).

[4] T.-C. Lu, T. H. Hsieh, and T. Grover, Detecting Topological Order at Finite Temperature using Entanglement Negativity, Phys. Rev. Lett. **125**, 116801 (2020).

[5] T.-C. Lu and S. Vijay, Characterizing long-range entanglement in a mixed state through an emergent order on the entangling surface, Phys. Rev. Research **5**, 033031 (2023).

[6] C. de Groot, A. Turzillo, and N. Schuch, Symmetry protected topological order in open quantum systems, Quantum **6**, 856 (2022).

[7] J. Y. Lee, Y.-Z. You, and C. Xu, Symmetry protected topological phases under decoherence, (2022), arXiv preprint ArXiv:2210.16323.

[8] J.-H. Zhang, Y. Qi, and Z. Bi, Strange correlation function for average symmetry-protected topological phases, (2022), arXiv preprint ArXiv:2210.17485.

[9] R. Ma and C. Wang, Average symmetry-protected topological phases s, (2022), arXiv preprint ArXiv:2209.02723.

[10] J. Behrends, F. Venn, and B. Béri, Surface codes, quantum circuits, and entanglement phases, (2022), arXiv preprint ArXiv:2212.08084.

[11] R. Fan, Y. Bao, E. Altman, and A. Vishwanath, Diagnostics of mixed-state topological order and breakdown of quantum memory, (2023), arXiv preprint ArXiv:2301.05689.

[12] Y. Bao, R. Fan, A. Vishwanath, and E. Altman, Mixed-state topological order and the errorfield double formulation of decoherence-induced transitions, (2023), arXiv preprint ArXiv:2301.05687.

[13] J. Y. Lee, C.-M. Jian, and C. Xu, Quantum criticality under decoherence or weak measurement, (2023), arXiv preprint ArXiv:2301.05238.
[14] Y. Zou, S. Sang, and T. H. Hsieh, Channeling Quantum Criticality, Phys. Rev. Lett. **130**, 250403 (2023).
[15] H. J. Briegel and R. Raussendorf, Persistent Entanglement in Arrays of Interacting Particles, Phys. Rev. Lett. **86**, 910 (2001).
[16] R. Raussendorf, S. Bravyi, and J. Harrington, Long-range quantum entanglement in noisy cluster states, Phys. Rev. A **71**, 062313 (2005).
[17] M. Aguado, G. K. Brennen, F. Verstraete, and J. I. Cirac, Creation, Manipulation, and Detection of Abelian and Non-Abelian Anyons in Optical Lattices, Phys. Rev. Lett. **101**, 260501 (2008).
[18] A. Bolt, G. Duclos-Cianci, D. Poulin, and T. M. Stace, Foliated Quantum Error-Correcting Codes, Phys. Rev. Lett. **117**, 070501 (2016).
[19] L. Piroli, G. Styliaris, and J. I. Cirac, Quantum Circuits Assisted by Local Operations and Classical Communication: Transformations and Phases of Matter, Phys. Rev. Lett. **127**, 220503 (2021).
[20] N. Tantivasadakarn, R. Thorngren, A. Vishwanath, and R. Verresen, Long-range entanglement from measuring symmetry-protected topological phases, (2021), arXiv preprint ArXiv:2112.01519.
[21] R. Verresen, N. Tantivasadakarn, and A. Vishwanath, Efficiently preparing GHZ, topological and fracton states by measuring cold atoms, (2021), arXiv preprint ArXiv:2112.03061.
[22] S. Bravyi, I. Kim, A. Kliesch, and R. Koenig, Adaptive constant-depth circuits for manipulating non-Abelian anyons, (2022), arXiv preprint ArXiv:2205.01933.
[23] T.-C. Lu, L. A. Lessa, I. H. Kim, and T. H. Hsieh, Measurement as a Shortcut to Long-Range Entangled Quantum Matter, PRX Quantum **3**, 040337 (2022).
[24] N. Tantivasadakarn, R. Verresen, and A. Vishwanath, The shortest route to non-Abelian topological order on a quantum processor, (2022), arXiv preprint ArXiv:2209.03964.
[25] N. Tantivasadakarn, A. Vishwanath, and R. Verresen, Hierarchy of Topological Order From Finite-Depth Unitaries, Measurement, and Feedforward, PRX Quantum **4**, 020339 (2023).
[26] M. Iqbal, N. Tantivasadakarn, T. M. Gatterman, J. A. Gerber, K. Gilmore, D. Gresh, A. Hankin, N. Hewitt, C. V. Horst, and M. Matheny, *et al.*, Topological order from measurements and feed-forward on a trapped ion quantum computer, (2023), arXiv preprint ArXiv:2302.01917.
[27] M. Foss-Feig, A. Tikku, T.-C. Lu, K. Mayer, M. Iqbal, T. M. Gatterman, J. A. Gerber, K. Gilmore, D. Gresh, and A. Hankin, *et al.*, Experimental demonstration of the advantage of adaptive quantum circuits, (2023), arXiv preprint ArXiv:2302.03029.
[28] J. Y. Lee, W. Ji, Z. Bi, and M. Fisher, Decoding measurement-prepared quantum phases and transitions: From Ising model to gauge theory, and beyond, (2022), arXiv preprint ArXiv:2208.11699.
[29] G.-Y. Zhu, N. Tantivasadakarn, A. Vishwanath, S. Trebst, and R. Verresen, Nishimori's cat: Stable long-range entanglement from finite-depth unitaries and weak measurements, (2022), arXiv preprint ArXiv:2208.11136.
[30] X. Chen, Z.-C. Gu, and X.-G. Wen, Classification of gapped symmetric phases in one-dimensional spin systems, Phys. Rev. B **83**, 035107 (2011).
[31] X. Chen, Z.-C. Gu, and X.-G. Wen, Complete classification of one-dimensional gapped quantum phases in interacting spin systems, Phys. Rev. B **84**, 235128 (2011).
[32] X. Chen, Y.-M. Lu, and A. Vishwanath, Symmetry-protected topological phases from decorated domain walls, Nat. Commun. **5**, 3507 (2014).
[33] A. Peres, Separability Criterion for Density Matrices, Phys. Rev. Lett. **77**, 1413 (1996).
[34] M. Horodecki, P. Horodecki, and R. Horodecki, Separability of mixed states: Necessary and sufficient conditions, Phys. Lett. A **223**, 1 (1996).
[35] J. Eisert and M. B. Plenio, A comparison of entanglement measures, J. Mod. Opt. **46**, 145 (1999).
[36] G. Vidal and R. F. Werner, Computable measure of entanglement, Phys. Rev. A **65**, 032314 (2002).
[37] M. B. Plenio, Logarithmic Negativity: A Full Entanglement Monotone That is Not Convex, Phys. Rev. Lett. **95**, 090503 (2005).
[38] For nonfixed-point SPTs, Ref. [20] provides numerical evidence that measuring the Heisenberg spin-1 chain, an SPT protected by $\mathbb{Z}_2 \times \mathbb{Z}_2$ symmetry of π rotations, leads a GHZ-type long-range order.
[39] L. Savary and L. Balents, Quantum spin liquids: A review, Rep. Prog. Phys. **80**, 016502 (2016).
[40] Y. Zhou, K. Kanoda, and T.-K. Ng, Quantum spin liquid states, Rev. Mod. Phys. **89**, 025003 (2017).
[41] C. Gross and W. S. Bakr, Quantum gas microscopy for single atom and spin detection, Nat. Phys. **17**, 1316 (2021).
[42] H. V. Kruis, I. P. McCulloch, Z. Nussinov, and J. Zaanen, Geometry and the hidden order of Luttinger liquids: The universality of squeezed space, Phys. Rev. B **70**, 075109 (2004).
[43] B. A. Bernevig, *Topological Insulators and Topological Superconductors* (Princeton University Press, Princeton, 2013).
[44] S. M. Girvin and A. H. MacDonald, Off-Diagonal Long-Range Order, Oblique Confinement, and the Fractional Quantum Hall Effect, Phys. Rev. Lett. **58**, 1252 (1987).
[45] T. Klein Kvorning, C. Spånslätt, A. P. O. Chan, and S. Ryu, Nonlocal order parameters for states with topological electromagnetic response, Phys. Rev. B **101**, 205101 (2020).
[46] C. H. Bennett, D. P. DiVincenzo, J. A. Smolin, and W. K. Wootters, Mixed-state entanglement and quantum error correction, Phys. Rev. A **54**, 3824 (1996).
[47] This implies that the connected correlation between two distant operators O_A, O_B is upper bounded by $\exp(-d/\xi)$ where d is the separation between O_A, O_B, and ξ is a finite correlation length.
[48] Namely, $SO_jS^\dagger = e^{iQ_j}O_j$ with $Q_j \bmod 2\pi \neq 0$ for $j = 1, 2$.
[49] This follows from the fact the eigenspectrum of the unitary S is located on the unit circle in the complex plane.
[50] S. Bravyi, M. B. Hastings, and F. Verstraete, Lieb-Robinson Bounds and the Generation of Correlations and Topological Quantum Order, Phys. Rev. Lett. **97**, 050401 (2006).
[51] F. Pollmann and A. M. Turner, Detection of symmetry-protected topological phases in one dimension, Phys. Rev. B **86**, 125441 (2012).

[52] $c = 1$ in the ground state of cluster state Hamiltonian.
[53] For instance, sequentially applying U_{CZ}, KW duality, U_{CZ}, one finds $X_{b,i} \to Z_{a,i}X_{b,i}Z_{a,i+1} \to Z_{a,i}X_{b,i}Z_{a,i+1} \to X_{b,i}$, and $Z_{a,i}Z_{a,i+1} \to Z_{a,i}Z_{a,i+1} \to X_{b,i} \to Z_{a,i}X_{b,i}Z_{a,i+1}$.
[54] L. Li, M. Oshikawa, and Y. Zheng, Non-invertible duality transformation between SPT and SSB phases, (2023), arXiv preprint ArXiv:2301.07899.
[55] In fact, at the critical point $g = 1$, $H = UH_0U^\dagger = H_0$, so $|\psi_0\rangle$ is the same as $|\psi\rangle$ defined in Eq. (10).
[56] C. Holzhey, F. Larsen, and F. Wilczek, Geometric and renormalized entropy in conformal field theory, Nucl. Phys. B **424**, 443 (1994).
[57] P. Calabrese and J. Cardy, Entanglement entropy and quantum field theory, J. Stat. Mech.: Theory Experiment **2004**, P06002 (2004).
[58] For a pure 1+1D CFT, α is a universal number related to central charges, and $\alpha = 1/4$ for Ising CFT [94]. The mismatch between 1/4 and 0.30 is attributed to finite-size effects.
[59] Z.-C. Gu and X.-G. Wen, Symmetry-protected topological orders for interacting fermions: Fermionic topological nonlinear σ models and a special group supercohomology theory, Phys. Rev. B **90**, 115141 (2014).
[60] C. W. von Keyserlingk and S. L. Sondhi, Phase structure of one-dimensional interacting floquet systems. I. Abelian symmetry-protected topological phases, Phys. Rev. B **93**, 245145 (2016).
[61] N. Tantivasadakarn and A. Vishwanath, Full commuting projector hamiltonians of interacting symmetry-protected topological phases of fermions, Phys. Rev. B **98**, 165104 (2018).
[62] U. Borla, R. Verresen, J. Shah, and S. Moroz, Gauging the Kitaev chain, SciPost Phys. **10**, 148 (2021).
[63] M. C. Gutzwiller, Effect of Correlation on the Ferromagnetism of Transition Metals, Phys. Rev. Lett. **10**, 159 (1963).
[64] F. D. M. Haldane, Exact Jastrow-Gutzwiller Resonating-Valence-Bond Ground State of the Spin-$\frac{1}{2}$ Antiferromagnetic Heisenberg Chain with $1/r^2$ Exchange, Phys. Rev. Lett. **60**, 635 (1988).
[65] B. S. Shastry, Exact Solution of an $s = 1/2$ Heisenberg Antiferromagnetic Chain with Long-Ranged Interactions, Phys. Rev. Lett. **60**, 639 (1988).
[66] X.-G. Wen, *Quantum Field Theory of Many Body Systems: From the Origin of Sound to an Origin of Light and Electrons* (OUP, Oxford, 2004).
[67] A. Kitaev, Anyons in an exactly solved model and beyond, Ann. Phys. **321**, 2 (2006). january Special Issue,
[68] Z. Zhang and S. Vijay, Forthcoming.
[69] I. Affleck, T. Kennedy, E. H. Lieb, and H. Tasaki, Rigorous Results on Valence-Bond Ground States in Antiferromagnets, Phys. Rev. Lett. **59**, 799 (1987).
[70] F. D. M. Haldane, Nonlinear Field Theory of Large-Spin Heisenberg Antiferromagnets: Semiclassically Quantized Solitons of the One-Dimensional Easy-Axis Néel State, Phys. Rev. Lett. **50**, 1153 (1983).
[71] M. den Nijs and K. Rommelse, Preroughening transitions in crystal surfaces and valence-bond phases in quantum spin chains, Phys. Rev. B **40**, 4709 (1989).
[72] The nonlocal string order of a single fermion chain can be mapped to the two-point function $(X_i + iY_i)(X_j - iY_j)$ of the spin-1/2 XY model $H = -\sum_i(X_iX_{i+1} + Y_iY_{i+1})$ via the Jordan-Wigner transformation. Since it is known that the two-point $\langle X_iX_j\rangle = \langle Y_iY_j\rangle \sim 1/\sqrt{|i-j|}$ in the XY model [95], the string order of fermion chain obeys that same scaling as well.
[73] A. J. Friedman, C. Yin, Y. Hong, and A. Lucas, Locality and error correction in quantum dynamics with measurement, (2022), arXiv preprint ArXiv:2206.09929.
[74] G. Vidal, Entanglement monotones, J. Mod. Opt. **47**, 355 (2000).
[75] Y.-X. Wang, L.-Z. Mu, V. Vedral, and H. Fan, Entanglement Rényi α entropy, Phys. Rev. A **93**, 022324 (2016).
[76] T. Kennedy and H. Tasaki, Hidden symmetry breaking and the haldane phase in$S$=1 quantum spin chains, Commun. Math. Phys. **147**, 431 (1992).
[77] T. Kennedy and H. Tasaki, Hidden $z_2 \times z_2$ symmetry breaking in haldane-gap antiferromagnets, Phys. Rev. B **45**, 304 (1992).
[78] M. Oshikawa, Hidden Z2*Z2 symmetry in quantum spin chains with arbitrary integer spin, J. Phys.: Condens. Matter **4**, 7469 (1992).
[79] Z. Ringel and S. H. Simon, Hidden order and flux attachment in symmetry-protected topological phases: A Laughlin-like approach, Phys. Rev. B **91**, 195117 (2015).
[80] More specifically, based on the condition that $P|\psi_0\rangle = |\psi_0\rangle$ and $P|\psi\rangle = |\psi\rangle = U|\psi_0\rangle$, where P is a projector to the subspace with $\prod_i X_{a,i} = \prod_i X_{b,i} = 1$, the eigenequation $H_0|\psi_0\rangle = E_g|\psi_0\rangle$ implies $PUHU^\dagger P|\psi\rangle = E_g|\psi_0\rangle$, so the parent Hamiltonian of $|\psi\rangle$ is $PUHU^\dagger P$.
[81] J. K. Pachos and M. B. Plenio, Three-Spin Interactions in Optical Lattices and Criticality in Cluster Hamiltonians, Phys. Rev. Lett. **93**, 056402 (2004).
[82] A. C. Doherty and S. D. Bartlett, Identifying Phases of Quantum Many-Body Systems that are Universal for Quantum Computation, Phys. Rev. Lett. **103**, 020506 (2009).
[83] T. Scaffidi, D. E. Parker, and R. Vasseur, Gapless Symmetry-Protected Topological Order, Phys. Rev. X **7**, 041048 (2017).
[84] This can also be understood in a dual picture, where the domain-wall creation operator in the trivial phase of Ising model correspond to a Wilson loop in the deconfined phase of the $2+1$D $\mathbb{Z}_2$ gauge theory, thereby following a perimeter law.
[85] For example, in the ground state of a $\mathbb{Z}_2$ gauge theory, such an operator follows an area-law decay as e^{-uLd} with u being an $O(1)$ constant.
[86] H. W. J. Blöte and Y. Deng, Cluster Monte Carlo simulation of the transverse Ising model, Phys. Rev. E **66**, 066110 (2002).
[87] A. Y. Kitaev, Unpaired Majorana fermions in quantum wires, Phys.-Usp. **44**, 131 (2001).
[88] J. Alicea, Majorana fermions in a tunable semiconductor device, Phys. Rev. B **81**, 125318 (2010).
[89] The basis state $|\beta\rangle$ corresponds to the $(c_2^\dagger)^{(1-\beta_2)/2}(c_4^\dagger)^{(1-\beta_4)/2}\cdots|0\rangle$, where $|0\rangle$ is the fermionic vacuum.
[90] U is a unitary in the $\mathbb{Z}_2 \times \mathbb{Z}_2^f$ symmetric subspace.
[91] This is in contrast to invertible fermionic topological order in Kitaev chain, which does not host fractionalized excitations in the bulk, and can be trivialized by stacking another copy of Kitaev chain.

[92] S. Vijay and L. Fu, Physical implementation of a majorana fermion surface code for fault-tolerant quantum computation, Phys. Scr. **2016**, 014002 (2016).

[93] Such basis can be written as the linear combination of the fermion occupation-number basis $(c_{1,\uparrow}^{\dagger})^{n_{1,\uparrow}}(c_{1,\downarrow}^{\dagger})^{n_{1,\downarrow}}(c_{2,\uparrow}^{\dagger})^{n_{2,\uparrow}}(c_{2,\downarrow}^{\dagger})^{n_{2,\downarrow}}\cdots|0\rangle$ with $|0\rangle$ being the fermionic vacuum.

[94] P. Calabrese, J. Cardy, and E. Tonni, Entanglement negativity in extended systems: a field theoretical approach, J. Stat. Mech.: Theory Experiment **2013**, P02008 (2013).

[95] B. M. McCoy, Spin correlation functions of the $x-y$ model, Phys. Rev. **173**, 531 (1968).